Received: 9 April 2023 | Accepted: 24 September 2023

DOI: 10.1002/bmm2.12056

REVIEW

BMEMat WILEY

Bio-inspired photonic crystals: Tailoring the dielectric building blocks to control the light propagation

Cun Zhu[1] | Lei Tian[2] | Wei Cheng[3] | Zhongze Gu[1]

[1]State Key Laboratory of Digital Medical Engineering, School of Biological Science and Medical Engineering, Southeast University, Nanjing, China

[2]Department of Chemical Engineering, McMaster University, Hamilton, Ontario, Canada

[3]Department of Chemical and Biochemical Engineering, University of Iowa, Iowa City, Iowa, USA

Correspondence
Cun Zhu and Zhongze Gu.
Email: czhu@seu.edu.cn and gu@seu.edu.cn

Funding information
National Key R&D Program of China, Grant/Award Number: 2017YFA0700500; 111 Project, Grant/Award Number: B17011; Natural Science Foundation of Jiangsu Province, Grant/Award Number: BK20202013

Abstract

Photonic crystals have drawn tremendous attention in recent years owing to their unique optical properties and remarkable advantages in various applications such as bioassays, sensors and optical devices. Benefiting from the spatially ordered structures, the flow of visible light can be manipulated by photonic crystals in a controlled manner. In this review, we summarize recent progress toward bio-inspired photonic crystals, including techniques for the construction of spatially ordered structures in diverse dimensions for photonic crystals, and strategies to manipulate the periodicity of the dielectric building blocks to control the light propagation in the presence of external stimuli. We start with the description of structure induced colors in nature with a systematic investigation to reveal the derivation of these colors, followed by a discussion on the design and fabrication of various types of bio-inspired photonic crystals by manipulating the arrangement of dielectric building blocks. We also highlight the stimuli responsive photonic crystals with tunable optical properties and their applications in sensing and color display.

KEYWORDS
bio-inspired, photonic crystal, responsive, structural color, tunable

1 | INTRODUCTION

During the long period of evolution, nature has created a wide variety of inexhaustible wealth to mankind. One of the most amazing miracles provided by nature is the color, which makes human beings live in a wonderful world filled with astonishing diversity. A huge number of inorganic substances, such as gemstones and metals, as well as living organisms including plants and animals (e.g., birds, fish, and insects) in nature have the ability to display various kinds of vivid colors. With the help of color, living creatures can fit perfectly with the surrounding environment to stay away from predators or use it as a signal to deliver information toward companions. Therefore, the mystery and origination of brilliant iridescent colors in nature have drawn great interests and become one of the research hotspots for centuries.

During the last several decades, tremendous effort has been directed toward the construction of functional materials and devices that can confine the transmission of light with particular wavelength and control the direction of light propagation through duplicating or mimicking

This is an open access article under the terms of the Creative Commons Attribution License, which permits use, distribution and reproduction in any medium, provided the original work is properly cited.

© 2023 The Authors. *BMEMat* published by John Wiley & Sons Australia, Ltd on behalf of Shandong University.

the living creatures in nature, especially those extraordinary geometric structures resided on living creatures for the exhibition of vivid colors. Photonic crystals, one kind of well-known artificial materials with spatially ordered structures that inspired from nature, have been proved as high-efficient photo-functional materials to generate brilliant colors. Due to the periodical arrangement of the dielectric building blocks in photonic crystals, one unique property known as photonic stop band (or photonic band gap) appears, leading to the prohibition of light with a certain wavelength or frequency located in the stop band to propagate through the photonic crystals.[1–7] As a result, distinct color in accordance with the frequency of reflected light will be observed, making it possible to manipulate the flow of light in a controlled fashion. According to the dimension of periodically aligned dielectric building blocks, photonic crystals can be mainly divided into three types, including one dimensional (1D), two dimensional (2D) and three-dimensional (3D) photonic crystals.

Since photonic crystals have shown remarkable advantages as an attractive photo-functional material for manipulating the flow of light, recent years have witnessed considerable efforts devoted to duplicate, mimic, design, and utilize the photonic crystals with a variety of compositions, scales and dimensions. Plenty of techniques have been developed to fabricate the photonic crystals and control the arrangement of dielectric building blocks, with notable examples including holographic lithography, electrochemical etching, layer-by-layer stacking, chemical vapor deposition, 3D printing, and self-assembly technique. Monodisperse colloidal nanoparticles, inorganic nanocrystals, polymers, and macromolecules can be used as building blocks for the construction of spatially ordered structures for photonic crystals. It should be emphasized that the photonic stop band of the resultant ordered structures fundamentally relies on the refractive index and periodicity of the dielectric building blocks. Therefore, it is possible to modulate the optical properties of photonic crystals by either changing the optical distance between adjacent building blocks, or controlling the average refractive index by doping certain components into or removing them from the spatial ordered structures. Moreover, the incorporation of responsive materials (e.g., elastomer, magnetic nanoparticles) brings the stimulus-responsive property to photonic crystals, resulting in a tunable photonic stop band that can effectively expand their practical applications not only in reflective coatings, waveguides, bioassays but also in novel responsive optical sensors and display devices.

In this review, we will provide a recent research progress in regard to bio-inspired photonic crystals, including techniques for the design and fabrication of photonic crystal in diverse scales and dimensions, and strategies for the manipulation of light propagation by tailoring the arrangement and periodicity of the dielectric building blocks. We first outline the strategies used by living creatures in nature for the generation of vivid iridescent colors, together with structural analysis to reveal the origination and mechanism of these colors. We then focus on a variety of techniques for the fabrication of spatially ordered structures for high-quality photonic crystals. The strategies for modulating the dielectric building blocks thus the photonic stop band to achieve tunable colors in the presence of external stimuli, and the applications of these responsive photonic crystals in sensing and display will also be highlighted. Finally, a summary and outlook about the prospect and opportunity for bio-inspired photonic crystals will be given. It should be noticed that all the examples described here are just a subset of what researchers have achieved in recent years owing to a growing number of novel techniques developed for the fabrication and application of photonic crystals. For additional information, please refer to cited references and previous reviews.[8–21]

2 | COLORS IN NATURE: FROM PHENOMENA TO PRINCIPLES

Colors in nature can mainly be divided into two types according to their generation, which are recognized as pigmentary color and structural color. The pigmentary color usually depends on natural pigments or chemical chromophores secreted by certain cells located on the surface or skin of the living creatures, which can control the reflection or transmission of visible light through wavelength-selective absorption. It has been found that the electron transitions occurring among the molecular orbitals play a key role in achieving such color. It should be noted that the vast majority of natural pigments or chemical chromophores are sensitive to surrounding environmental conditions such as temperature, humidity or light intensity, which might affect the distribution or even molecular structures of these pigments or chromophores, eventually leading to fading of exhibited colors. On the other hand, the structural color mainly relies on the physical geometric structures constructed by reflective building units for the color exhibition. Thanks to its physical derivation, the structural color is much more stable and efficient in the use of light.

Although living creatures have created diverse strategies to develop their body color during several hundred million years of evolution, the most vivid color in nature is more or less derived from manipulating the

propagation of light in the visible region with the help of certain structures. According to the generation and mechanism, the structural colors in nature are considered to originate from thin film or multilayer interference, diffraction or scattering of visible light, or their combinations. In this section, we will focus on strategies that living creatures utilized for color exhibition, with notable examples of different types of structures to reveal the derivation and mechanism of these colors.

2.1 | Multilayer interference

Multilayer interference is with no doubt the most common and well-understood mechanism that living creatures used for the generation of vivid iridescent color. It usually takes place at a stack of thin films with high and low refractive indices that are arranged alternately. When light propagates through such a stack, some of the light is reflected from both the top and bottom boundaries of each thin film layer. The reflected light from the bottom boundary will travel back and rejoin those reflected from the top of this layer. These two parts of reflected lights may have different phases owing to the differences in the thickness and refractive index of the two adjacent layers, eventually resulting in the generation of a particular color. Multilayer interference is particularly common in invertebrates such as insects, worms, shrimps and octopuses, which is usually produced by periodic secretion and deposition at the cellular level.

According to the arrangement of stacked layers, there are several different types of multilayer interference utilized by living creatures in nature: (1) quarter-wave stack, a regular multilayer system formed by a stack of thin film layers with optical thickness tuned to a specific value. The *Chrysochroa fulgidissima*, a distinctive jewel beetle in Japan, displays glittering yellowish green color using such stack (Figure 1a). It has been found that more than a dozen alternate layers with different refractive indices parallelly arranged under its outer side, which are responsible for the generation of their body color.[22,31] (2) Chirped stack, a multilayer system containing thin films with optical thicknesses gradually increased or decreased. Different color can be reflected at different depths, leading to a broadband reflectance. For instance, the golden body color of chrysalis in the genera *Euoplea* originates from this kind of stack located on their surface (Figure 1b).[23] (3) Chaotic stack, a stack of disordered or randomly arranged layers with thicknesses about a mean value. The compound eyes of *Astacus* (Figure 1c), a typical example that formed by a multilayer of isoxanthopterin crystals with irregular thickness and arrangement, can exhibit distinct color.[24] Those layers in such stacks serve as mirrors to reflect most or all wavelengths of visible light simultaneously. (4) Helical stack, a stack of layers helically arranged with successive rotations to only reflect circular waves of inverse chirality.[32] Such multilayer-based iridescent color can be found in plants such as the marble berries of *Pollia condensate* (Figure 1d). In the cell walls of the epicarp, it has been discovered that multilayers formed by helicoidally stacked cellulose microfibrils are crucial for the generation of the polarized reflected light and strong iridescent color.[25] Since the layer thickness in such stacks varies from cell to cell, leading to a pixelated color of each cell thus a pointillist appearance. The flower beetle *Chrysina resplendens* also develop their body color by utilizing this mechanism.[33]

2.2 | Grating diffraction

A grating for diffraction is an array with periodic structures composed of parallel ridges, grooves, or slits that splits and diffracts light into several beams with its constituent wavelengths traveling in various directions deviated from the direction of simple reflection or transmission. The directions of the diffracted lights rely on the periodicity of the grating and the wavelength of light. When diffraction occurs after a continuous light transiting through the gratings, it can create rainbow-like colors in the whole visible region due to the diffraction of light with different wavelengths in different directions; thus, various colors can be observed at different viewing angles.

Iridescence generated through grating diffraction is quite common in a diversity of living creatures, especially in invertebrates such as worms, flies, butterflies, and some plants. For instance, it has been discovered that various colors can be observed under varying viewing angles on the first antenna of the seed-shrimp *Azygocypridina lowryi* (Figure 1e).[23,24] The appearance of such colors should be attributed to the gratings composed of paratactic rings with walls circular in cross section on their surfaces. Another notable example is the *Morpho* butterflies, a kind of well-known iridescent insect living in Central and South America that exhibit vivid iridescent color (Figure 1f).[26] It has been discovered that a large quantity of ordered hierarchical structures are located on both sides of the transparent epithelial membranes on their wings, which consist of parallelly aligned equidistant ridges and rows of periodical cross ribs. Both diffraction and multilayer interference take place simultaneously at these regularly arranged structures. However, the grafting diffraction from the ridges plays a key role in the brilliant color in most *Morpho* species.[34,35]

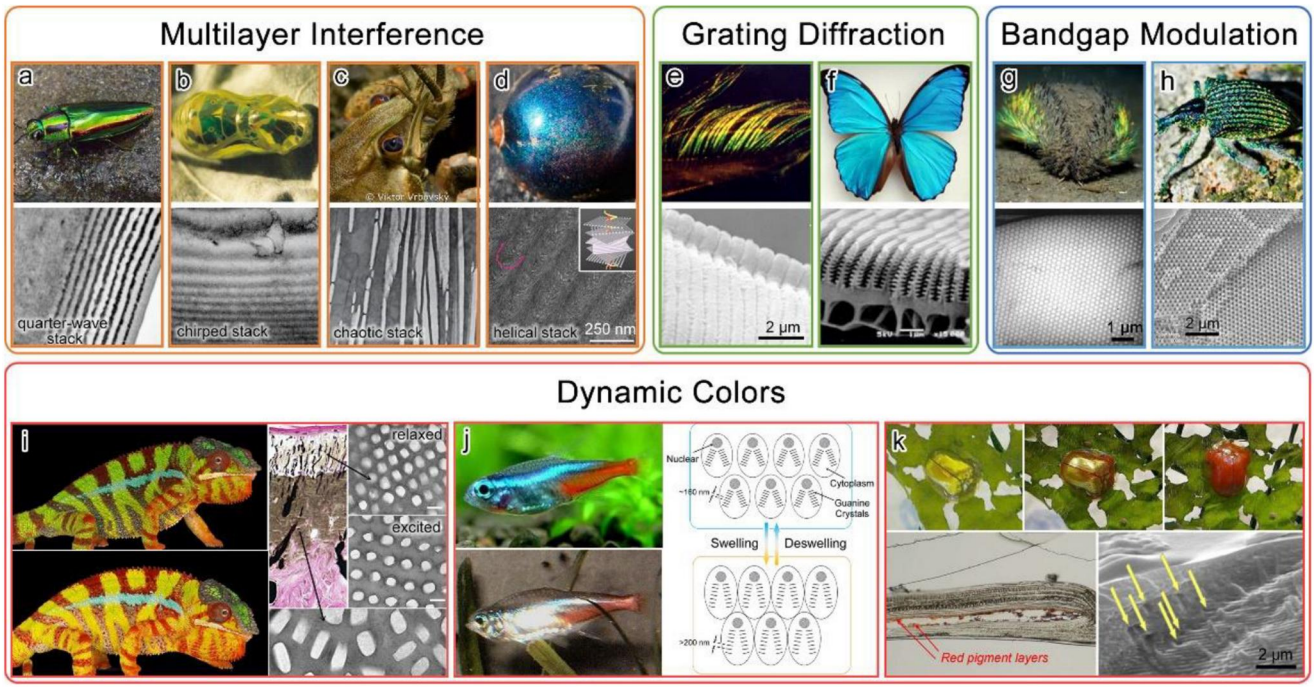

FIGURE 1 (a–d) Multilayer interference-based iridescent color in nature: (a) a quarter-wave stack used by the *Chrysochroa fulgidissima*,[22] Copyright 2008 IOP Publishing. (b) A chirped stack utilized by the chrysalis of butterfly *Euoplea*,[23] Copyright 2000 IOP Publishing. (c) A chaotic stack used by the compound eyes of *Astacus*,[24] Copyright 2006 Elsevier Ltd. (d) A helical stack used by the fruit of *Pollia condensate*,[25] Copyright 2012 Elsevier Ltd. (e,f) Living creatures utilize diffraction grating to develop their body color: (e) the hairs of the seed-shrimp *Azygocypridina lowryi*,[23,24] Copyright 2000 IOP Publishing. (f) The epithelial membrane of *Morpho* butterfly,[26] Copyright 2008 Wiley-VCH. (g,h) Animals use spatial ordered structures for color exhibition: (g) the hairs and spines of sea mouse *Aphrodita*,[27] Copyright 2003 Elsevier Ltd. (h) The elytron of weevil *Entimus imperialis*,[25] Copyright 2012 Elsevier Ltd. (i–k) Living creatures with tunable body colors in nature: (i) the *chameleon*,[28] Copyright 2015 Nature Publishing Group. (j) The fish *Paracheirodon innesi*,[29] Copyright 2011 Optica Publishing Group. (k) The adult leaf beetles *Charidotella egregia*.[30] Copyright 2007 American Physical Society.

Such structures can also be found in some flowering plants. White petals of *Hibiscus trionum* with a patch of red at the base emerge in blue, green, and yellow color according to viewing angles. Though the red color is produced by pigment, scanning electron microscopy image clearly reveals that ordered cuticular striations served as diffraction gratings overlaying the epidermal cells should be responsible for the iridescent color.[36]

2.3 | Bandgap modulation

Beyond multilayer structures and diffraction gratings, living creatures in nature have developed diverse techniques to utilize the visible light. Many species of animals have evolved spatial ordered structures on their surface, skin or feather to produce brilliant colors with the help of special crystalline structures. Such structures are typically composed of dielectrics with different refractive indexes that are periodically arranged in two or three dimensions, leading to the generation of a certain photonic bandgap to control the light propagation. For instance, the sea mouse *Aphrodita* appears beautiful iridescence on the hairs and spines located on the lower edge of its body (Figure 1g).[27] The electronmicroscopical study of the hairs and spines indicates that they both contain annular structures of holes aligned in a hexagonal packed fashion, which should be mainly responsible for the iridescent color. The peacock *Pavomuticus* is another typical example with a similar periodic structure to exhibit various vivid colors. An array of melanin rods is located under the surface keratin layer of the colored barbules, which generates diversified colors in their feathers.[37] In addition, it has been reported that the wings of the emerald-patterned cattleheart butterfly *Parides sesostris* contain gyroid-type laminae in the cover scale to produce the green color. These ordered structures are separated into multiple neighboring domains with different crystal orientations, resulting in the exhibited color completely independent of the viewing angle.[38–40] The Brazilian diamond weevil *Entimus imperialis*, longhorn beetle *Pseudomyagrus waterhousei*, and tropical weevil *Pachyrrhynchus congestus pavonius* also have the ability to utilize the spatial periodic structure for color

exhibition.[41,42] Take the first beetle for example, it has been discovered that the colored spots on their elytron contain face-centered cubic structures with a triangular lattice arrangement (Figure 1h). Each unit cell in the stack of chitin slabs includes one hole and one protrusion, and they assembled into regular domains with different orientations and sizes for color display.

2.4 | Dynamic colors in nature

Although living creatures in nature have utilized different strategies to develop various kinds of vivid colors, these colors are not always static. It is not difficult to find that many animals such as fish, cephalopods, insects, amphibians and other living creatures are able to control their body colors to adapt themselves to the surrounding environment for camouflage, signaling or thermoregulation. Generally, the change of body color can be realized by either slightly shrinking/stretching the surface layer of animals to effectively change the periodicity of specific regular arrays composed of light selective reflecting units, or dispersing/aggregating fluids or organelles containing chemicals such as pigments to the microstructures on the surface layer to modify the efficiency and selectivity of light reflection. These actions are sufficient to cause an obvious shift in the wavelength of reflected light and thus the exhibited iridescent color, regardless of the change in some cases being quite tiny.

Chameleons are one of the most notable animals that have the ability to dramatically and continuously change their body color in response to the surrounding environment for camouflage. It has been proved that the change in periodicity of light reflecting units should be associated with their dynamic body color.[28] The *chameleons* have evolved a combination of two superposed layers of iridophores with different morphologies and functions (Figure 1i). The upper multilayer contains iridophores with small non-close-packed guanine crystals organized in a triangular lattice, which are mainly responsible for the rapid color change through active tuning of the spacing among these guanine nanocrystals. Another adjacent deeper layer of iridophores containing larger guanine crystals can broadly reflect sunlight. Fish such as *Paracheirodon innesi* and *damselfish* also utilize a similar mechanism to control their body color. The tunable iridescent color in the lateral stripe should be attributed to the swelling or deswelling of the platelets, and the change in distance among periodically stacked guanine crystals inside the elliptic iridophore cells (Figure 1j).[29] In addition, the adult leaf beetles *Charidotella egregia* utilize another route to reversibly switch the color of their cuticle.[30] As demonstrated in Figure 1k, they can control the moisture of the multilayer reflector by injecting or removing a fluid at the bottom of their elytron into the upper porous multilayer to control the interference and absorption of light to realize the color change. Their golden body color arises from multilayer interference with the help of a chirped stack of thin film layers, which can quickly switch to red in the presence of external stimulus. The color change should be attributed to the expulsion of liquid from the upper porous multilayer, which will tune the multilayer into transparent and show a red color from deeper red pigment layers.

3 | BIO-INSPIRED PHOTONIC CRYSTALS: DESIGN AND FABRICATION

The brilliant iridescent color and unique structures utilized by living creatures in nature have attracted considerable attention for over centuries. Tremendous work has been conducted on the study of the mechanism of structural color and the imitation of these structures. Photonic crystals, one kind of bio-inspired photofunctional materials with highly designable and manageable spatial ordered structures, have emerged as a vital tool to realize the manipulation of light propagation and the exhibition of various brilliant colors. During the past several decades, plenty of techniques have been developed to fabricate bio-inspired photonic crystals with controlled optical properties. In general, photonic crystals with spatially ordered structures can be achieved by either "top-down" micromachining or "bottom-up" assembly; notable tactics include holographic lithography, laser-guided stereolithography, chemical vapor deposition, layer-by-layer stacking, and self-assembly techniques. Compared with top-down method that relies on photolithography and etching techniques, bottom-up assembly has been considered as a versatile and convenient strategy to control the alignment of dielectric building blocks owing to the avoidance of using expensive facilities and complex procedures. A variety of materials such as monodisperse colloidal nanoparticles with the size ranging from tens to hundreds of nanometers, metal nanocrystals, and macromolecules with well-defined structures can be utilized as building blocks for the construction of photonic crystals with diverse compositions and dimensions. Herein, we will highlight typical bottom-up techniques for the creation of photonic crystals with periodic structures in various scales and dimensions, including the self-assembly, physical deposition, printing assisted assembly, and field induced assembly technique. Table 1 provides an overview of the techniques described in the following.

TABLE 1 Overview of typical "bottom-up" techniques for the fabrication of high-quality bio-inspired photonic crystals.

Methods		Schematics	Building blocks	Descriptions	Remarks	References
Molecular self-assembly		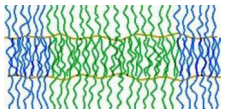	Polymers, macromolecules (e.g., block copolymers, cholesteric liquid crystals, surfactant molecules)	Molecules spontaneously organize into stacked lamellae containing alternative layers	Requires appropriate molecular weight or structure; large scale; uneven color	[43–45]
Multilayer stacking		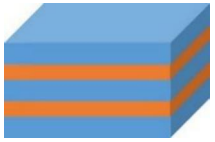	Polymers, colloidal nanoparticles (e.g., silica or polymer colloids)	Continuously deposit a set of alternative layers with varying refractive indices or thicknesses	Includes LbL, CVD, PLD, and spin coating; simple and fast; large scale; broader spectrum	[46–48]
Interfacial assembly		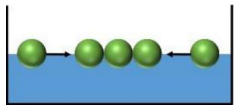	Colloidal nanoparticles	Colloids assemble into 2D ordered structures at the liquid-air or liquid-liquid interface	Requires volatile solvent for the dispersion of colloids; large scale; difficult to obtain 3D or complex structures; slow process	[49,50]
Physical deposition	Horizontal deposition	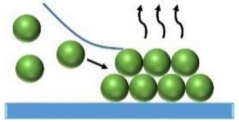	Colloidal nanoparticles	Colloids aggregate and self-assemble at the edge of liquid-air interface	Convenient and simple; easy patterning; coffee-ring effect may affect the long-range order	[51–53]
	Vertical deposition	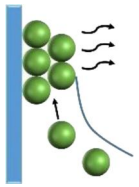	Colloidal nanoparticles	Colloids self-assemble at the edge of liquid-air interface on vertically placed substrates	Requires hydrophilic substrate and undisturbed environment; slow process	[54,55]
Physical confined assembly	Template confined assembly	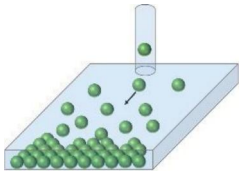	Colloidal nanoparticles	Colloids self-assemble in a confined space	Requires geometrical confined cells or substrates as template; topology manipulatable; limited scale; possibility of jamming	[56–58]

TABLE 1 (Continued)

Methods		Schematics	Building blocks	Descriptions	Remarks	References
	Droplet confined assembly	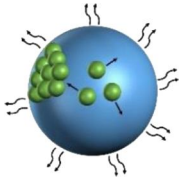	Colloidal nanoparticles	Colloids self-assemble at the interface of the liquid droplet	Requires microdroplets or microcapsules as template; risk of defects formation; limited scale	[59–61]
Printing assisted assembly	Ink-jet printing	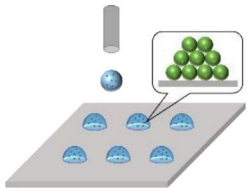	Hydrogel, resin, colloidal nanoparticles	Colloids self-assemble inside of the ink droplets on certain substrate	Requires proper solvent for printing ink and precise control of printing parameters; pattern manipulatable; time-consuming in large scale printing	[62,63]
	3D printing	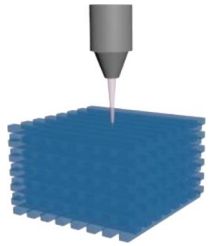	Hydrogel, resin, colloidal nanoparticles	Direct LbL stacking of the building blocks, or combine the bottom-up colloids self-assembly with top-down printing	Includes DIW, DLW, DLP; pattern manipulatable; limited scale	[64–67]
Field induced assembly	Electric field induced assembly	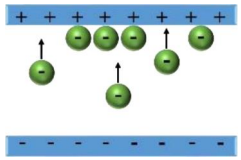	Charged colloidal nanoparticles	Charged colloids aggregate and assemble under an external electric field	Requires AC or DC field to induce the assembly; fast and tunable responsiveness; poor long-term stability	[68,69]
	Magnetic field induced assembly	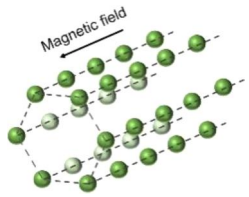	Magnetic colloidal nanoparticles	Magnetic colloids assemble into 1D chainlike structures under an external magnetic field	Requires magnetic field to induce the assembly; requires solution environment to maintain the tunability; rapid responsiveness; poor long-term stability	[70–72]

3.1 | Molecular self-assembly

Block copolymers have been considered as one of the ideal nanostructured materials for the construction of Bragg stacks because they have the ability to spontaneously self-assemble into ordered 1D microstructures through the microphase segregation of chemically different polymer blocks to generate a photonic stop band to control the light propagation.[43,44,73–78] For example, brush block copolymers can readily self-assemble into stacked lamellae with alternative layers of the different polymer blocks to enable the light reflection.[79] The emerged photonic stop band is determined by the domain sizes of different blocks, which can be precisely manipulated through controlling the relative incorporation of polymer components and blend of brush block copolymers. Swager and co-workers reported the fabrication of full-color reflective photonic ellipsoids by using the self-assembled dendronized brush block copolymers (den-BBCPs) as building blocks.[43] Two different dendronized surfactants with selective affinity to each block were utilized to modulate the interfacial properties of den-BBCPs and transform the shapes of den-BBCP particles from spheres to ellipsoids. The reflected color could be readily tuned within the entire visible spectrum by controlling the molecular weight of the block copolymers in a range from 477 to 1144 kDa (Figure 2a). Moreover, the orientation and alignment of the Fe_3O_4-functionalized hybrid photonic ellipsoids could be controlled by the external magnetic field, leading to dynamic color switching phenomenon between the on and off states. It is worth mentioning that the emulsion technique has also been successfully applied in the fabrication of photonic microspheres by using the bottlebrush block copolymers (BBCPs). The water-in-oil-in-water multiple emulsions stabilized by the BBCPs could spontaneously organize into ordered porous structures to reflect the visible light under a suitable range of interfacial tension. By simply adjusting the molecular weight of BBCPs, photonic microspheres with

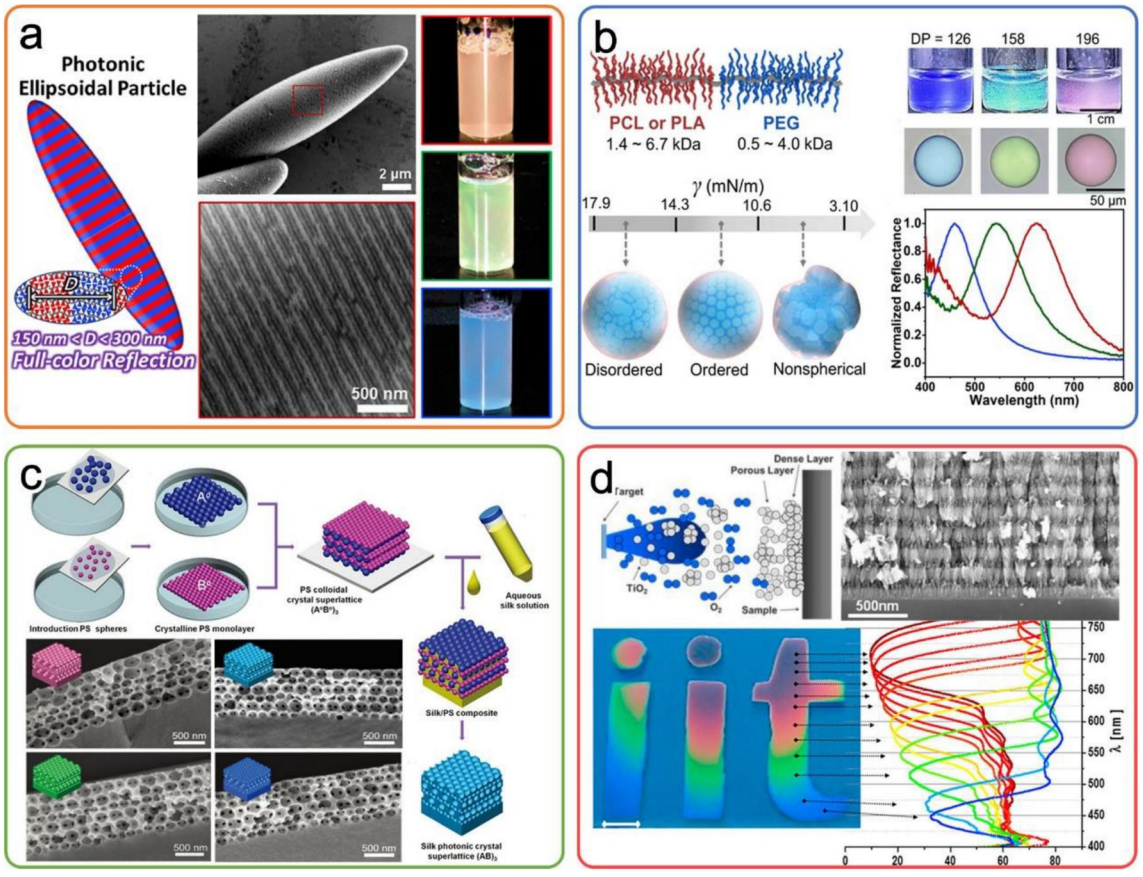

FIGURE 2 (a) Self-assembly of dendronized brush block copolymers into photonic ellipsoids with stop band across the entire visible spectrum.[43] Copyright 2020 American Chemical Society. (b) Porous photonic microspheres fabricated by the bottlebrush block copolymers using the emulsion technique.[44] Copyright 2022 Wiley-VCH. (c) Photonic crystal superlattices with inverse opal structures fabricated by LbL deposition.[46] Copyright 2018 Wiley-VCH. (d) Hierarchical Bragg stacks of TiO_2 multilayers with controlled porosity fabricated via the PLD technique.[48] Copyright 2014 American Chemical Society.

highly saturated structural colors covering the whole visible range had been achieved, as shown in Figure 2b.[44]

In addition to block copolymers, highly swollen lamellar structures with periodicity in hundreds of nanometers can be achieved by surfactant molecules to control the light propagation because surfactants have the ability to form a variety of self-assembled structures according to their concentrations in solution. It has been demonstrated that various brilliant iridescent colors could be clearly observed by a self-assembled nonionic surfactant n-dodecyl glyceryl itaconate (DGI) in the presence of a small amount of ionic surfactant sodium dodecyl sulfate (SDS).[45] The mixture of DGI and SDS self-assembled into stacks of bilayer lamellar sheets with an interval of submicrometers in water to generate a photonic stop band. The presented iridescent color in an equilibrium state could be readily modulated from red to deep blue by increasing the molar ratio of SDS to DGI due to the formation of separated onion-like or myelin-like structures as well as the decrease in spacing distance between bilayer membranes.

3.2 | Multilayer stacking

The multilayer stack has been considered as one of the most common and efficient structures evolved by nature for the generation of vivid colors; thus, biomimetic photonic materials consisting of periodic stacks of multiple layers have drawn considerable attention in recent years. Such multilayer stacks can be obtained via continuously depositing a set of alternative thin films with varying refractive indices and thicknesses on certain substrates, with motivation to achieve photon confinement and the selective transmission of visible light. Tremendous effect has been devoted to the design and fabrication of multilayer stacks during the past decades. Various techniques such as layer-by-layer (LbL) deposition, chemical vapor/solution deposition (CVD or CSD), pulsed laser deposition (PLD), and spin coating (or spin casting) have emerged as effective pathways to this objective.[46–48,80–86]

LbL deposition has been considered as a promising candidate for the alternate deposition of a pair of materials with opposite charges or colloidal nanoparticles with different sizes to construct the biomimetic multilayer stacks. As a typical example, large-scale photonic crystal superlattices formed by stacks of monolayer with different periodicities have been successfully produced for the effective diffraction of light.[46] The close-packed polystyrene (PS) monolayers that formed by PS nanoparticles with different diameters at the water/air interface were served as building blocks and stacked in a desired order, resulting in the formation of PS colloidal crystal superlattices. The subsequent introduction of aqueous silk solution into the void of the PS superlattices and removal of the PS nanoparticles using toluene eventually lead to the generation of silk photonic crystal superlattices with inverse opal structures (Figure 2c). Such superlattices were highly tunable by simply manipulating the ordering and periodicity of the PS template stacks, which exhibited excellent mechanical and optical properties. The PLD technique also provides a versatile route to the fabrication of multilayer stacks for color display. Fonzo and coworkers developed a high-efficiency Bragg reflector composed of TiO_2 multilayers with controlled porosity on various substrates.[48] The PLD technique was applied to generate photonic hierarchical nanostructures through alternatively depositing dense and porous TiO_2 layers as elementary building blocks based on the bottom-up strategy. They also demonstrated that patterned photonic crystals with successively changed photonic stop bands could be fabricated with a thickness gradient of the layers by utilizing a shadow mask, as shown in Figure 2d.

Spin coating has also been considered as a convenient and versatile technique for the fabrication of multilayer stacks. With the help of centrifugal force, the applied solution or suspension containing materials such as polymers or colloidal nanoparticles will spread over the substrate to form a smooth and uniform film. A multilayer stack will be obtained by alternately depositing two distinct components on the substrate via spin coating. Utilizing this technique, nanoparticle-based 1D photonic films had been fabricated as frequency selective filters for the incident radiation.[47] Spherical SiO_2 nanoparticles and irregular TiO_2 nanocrystals that present large differences in dielectric constant were served as functional components for the repeating units in the periodic multilayer stacks. By controlling the structural parameters such as spatial period of the refractive index, and relative thickness of the constituent layers, the resultant films appeared tunable photonic stop band. It should be noticed that spin coating is also capable of fabricating 2D or 3D photonic structures by depositing suspensions of monodisperse colloidal nanoparticles.

3.3 | Interfacial assembly

The assembly taking place at the liquid-air or liquid-liquid interface has proved to be a versatile strategy to fabricate photonic structures with various compositions and sizes because it provides a reliable and convenient route to restrict the arrangement of colloidal nanoparticles. A monolayer of 2D colloidal crystal array can be readily fabricated through the self-assembly of

monodisperse nanoparticles at the liquid-air interface utilizing the mechanism similar to the Langmuir-Blodgett (LB) technique.[46,87–92] During the fabrication, nanoparticles that dispersed in a volatile solvent (e.g., alcohol, chloroform, hexane) are introduced onto the water surface drop by drop. Driven by the gradient surface tension, the nanoparticle suspension subsequently spreads over the interface into an equilibrium state. After the evaporation of the solvent, a water-supported monolayer of nanoparticles will be obtained, which can be subsequently collected by desired substrates.

Following this mechanism, Asher and coworkers fabricated a large 2D colloidal crystal array at the water/air interface.[49] The alcohol suspension of nanoparticles was injected onto the water surface through a sharpened needle tip so as to form a 2D array over the entire water surface. The resultant 2D array could be conveniently transferred onto a solid substrate. A slight modification during the fabrication by removing the water layer after the formation of ordered 2D colloidal crystal arrays could yield such 2D arrays on diverse substrates. In their following work, large asymmetric 2D colloidal crystal array films have been successfully fabricated for the effective diffraction of light.[50] The introduction of a thin layer of tetraethyl orthosilicate (TEOS) onto the as-prepared 2D PS nanoparticle array caused the partial swollen and dissolution of the PS nanoparticles. After the evaporation of TEOS, a continuous asymmetric free-standing 2D film consisting of a hemispherical PS nanoparticle array on one side and fused flat PS layer on the other side could be obtained.

3.4 | Physical deposition

3.4.1 | Horizontal deposition

The horizontal deposition has been considered as one of the most convenient and versatile methods to generate 3D crystalline lattice, which involves several complex processes including Brownian motion, gravitational settling and crystallization. Typically, the horizontal deposition of colloidal nanoparticles is driven by the evaporation of solvent and capillary flow. It will be beneficial for the fabrication of photonic structures by carefully controlling parameters such as settling velocity and evaporation rate, as well as the density, concentration, and size of the colloidal nanoparticles. Despite the simplicity of this method, it is quite difficult to control the quality of the obtained structures because it usually involves the formation of vacancies, cracks, and polycrystalline domains of uncontrollable sizes and thicknesses. In addition, the coffee-ring effect will cause uneven distribution of colloidal nanoparticles after the evaporation and reduce the quality of resultant structures. Thus, the sedimentation process should be carefully controlled for the crystallization to form lattices with well-ordered structures.

In order to obtain colloidal crystal films with high quality in large scale and short period of time, several strategies have been developed on the basis of horizontal deposition.[93,94] Fudouzi reported a simple method for the fabrication of large-scale uniform opal films in the presence of hydrophobic silicone liquid.[51,95] It has been revealed that colloidal nanoparticles trend to aggregate and assemble at the edge of liquid-air interface to form a coffee-ring shaped structure due to a faster evaporation rate at the edge, as well as the capillary flow from bulk to edge of the suspension.[96–98] Covering the suspension with the silicone liquid effectively reduced the evaporation rate to prevent the capillary flow, thus high quality opal films free from the ring structures could be obtained.

In addition, the scalable fabrication of 3D highly ordered colloidal crystals can also be realized by the doctor blade coating technique using the principle of horizontal deposition.[52,99,100] An immobilized blade vertically settled to the substrate is utilized to provide a unidirectional shear force to the nanoparticle suspension. With the help of capillary force, colloidal nanoparticles self-assemble into periodic structures when they pass through the small gap between the blade and the substrate, as shown in Figure 3a. The fabrication speed and thickness of the resultant opal structures can be conveniently adjusted by parameters including the evaporation rate and viscosity of the colloidal suspension.

It has to be mentioned that the melt-shear organization technique has emerged as a promising candidate for the fabrication of opal films with spatially ordered structures in recent years.[53,101–103] Monodisperse colloidal latexes with hard cores composed of either inorganic nanoparticles or crosslinked organic nanoparticles, and soft shells composed of elastic polymers (e.g., poly(ethyl acrylate), poly(butyl acrylate)) are usually utilized as building blocks for the fabrication of such opal films. These core-shell colloidal latexes have the ability to merge and self-assemble into ordered structures by increasing the temperature slightly above their glass transition temperature and applying uniaxial pressure in a microextruder. The hard cores of these colloidal latexes can preserve their shape in the flowing melt during this process, while the elastomeric shells keep the ability to permit flow in the melt. As a result, crystalline layers of the colloidal latexes can be constantly deposited along the plates of the press, eventually leading to the formation of opal films with distinct structural color.

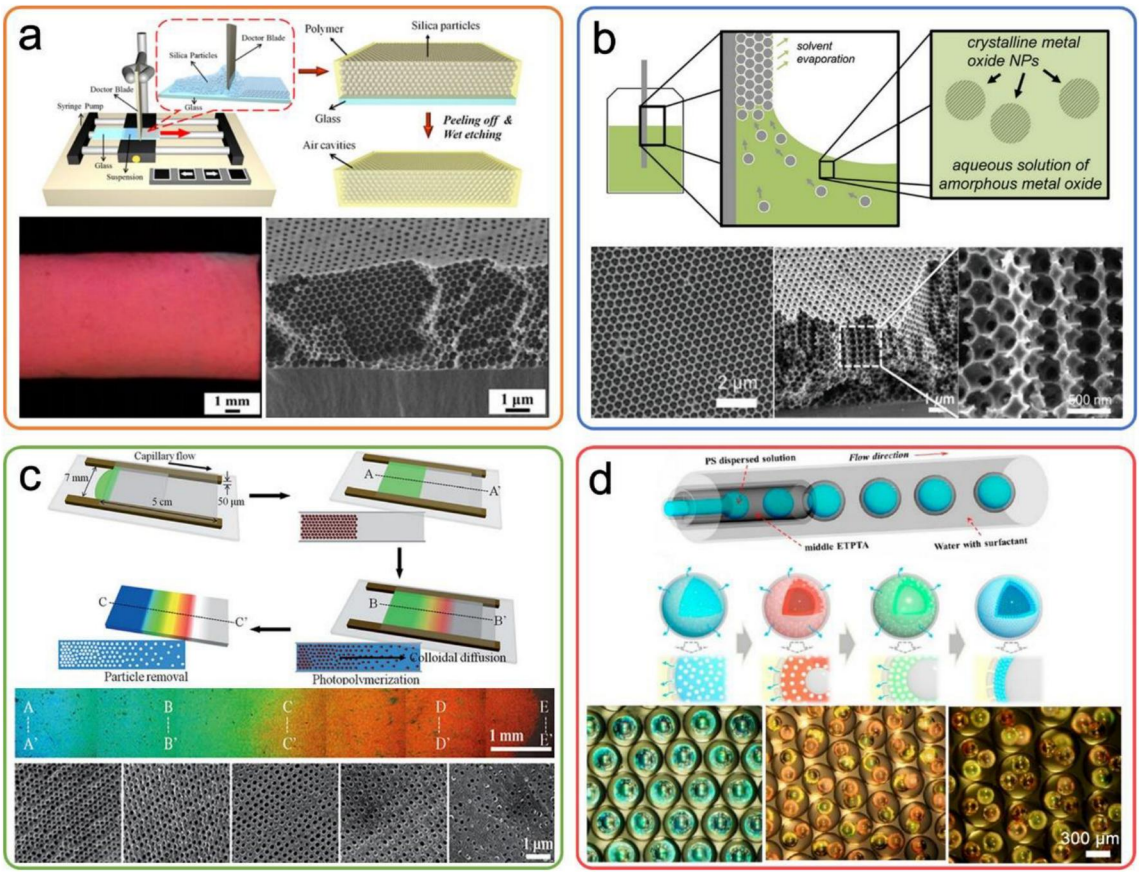

FIGURE 3 (a) Photonic crystals fabricated through a doctor blade coating technique.[52] Copyright 2020 American Chemical Society. (b) Metal oxide inverse opal films fabricated via evaporation-induced vertical deposition.[54] Copyright 2018 Wiley-VCH. (c) A chirped opal film obtained from confined assembly of colloids in a microchannel.[58] Copyright 2011 Wiley-VCH. (d) Confined self-assembly of colloidal nanoparticles inside of the double emulsion droplets.[61] Copyright 2015 American Chemical Society.

3.4.2 | Vertical deposition

Similar to the horizontal deposition, colloidal nanoparticles can also form closely packed ordered structures in diverse dimensions on the surface of vertically placed substrates (e.g., glass slides, capillaries). Driven by the capillary force, colloidal nanoparticles spontaneously self-assemble at the liquid-air interface to form periodic structures to control the propagation of light. The dip-coating is the simplest way to achieve the vertical deposition, where a clean wettable substrate is dipped into the colloid suspension vertically or with a small angle.[104–107] With the assistance of capillary force, the evaporation of the solvent will initiate and maintain the continuous deposition and growth of the crystal lattice at the interface. Aizenberg et al. fabricated metal oxide inverse opal films by co-assembling the template colloidal nanoparticles together with a metal oxide precursor via evaporation-induced vertical deposition, as shown in Figure 3b. Using the co-assembly, it is possible to incorporate functional nanoparticles such as gold nanoparticles into the inverse opal matrix to obtain highly ordered hybrid inverse opal films with homogeneously distributed functional nanoparticles.[54]

It is worth noting that the vertical deposition of colloidal nanoparticles on a stationary substrate may suffer from a relatively slow rate due to the slow evaporation of the solvent. Hence, a lifting method has been established to enhance the deposition. Utilizing this strategy, colloidal crystals with a close-packed face-centered-cubic (fcc) lattice and the (111) facet parallel to the substrate can be readily fabricated by carefully withdrawing the substrate from the colloidal suspension at a controlled speed.[55,108,109] Thanks to the constant lifting velocity, the thickness of obtained film is relatively uniform, which can be conveniently modulated from a single layer to multiple layers by precisely controlling the lifting velocity and the concentration of colloidal suspension. Moreover, the revealed photonic stop band and structural color can be simply modulated by the size of colloidal nanoparticles used as building blocks.

3.5 | Physical confined assembly

3.5.1 | Template confined assembly

Though horizontal and vertical depositions play the predominant role in the fabrication of spatially ordered structures, it is still a challenge to manipulate the topology of generated photonic structures. To solve this problem, a versatile technique known as template-confined assembly has been developed. By utilizing this strategy, various controllable photonic structures including opal films, stripes, trenches, even stacks of nanoparticles with controlled combinations and morphologies can be readily fabricated.[110,111] The addition of external force such as pressure, capillary force, or gravity may promote this process and accelerate the deposition rate of the photofunctional building blocks. Xia reported the rapid fabrication of crystalline lattices over large areas in a confined cell.[56] The continuous injection of nanoparticle suspension into the cell provided a positive pressure to force the solvent flow through the channels at the bottom of the cell. As a result, the introduced nanoparticles self-assembled into a close-packed lattice under continuous sonication. In their following works, they utilized the geometrical confined cell to achieve the assembly of colloidal nanoparticles into specific structures such as polygonal homoaggregates, trenches,[57,112] and even hetero-aggregates such as asymmetric dimers.[113] Marlow and coworker used a planar capillary cell equipped with a capillary tube to prepare opal films from stable nanoparticle suspension. The suspension was transported into the capillary cell with the help of capillary force to realize the confined assembly of PS nanoparticles.[114] Moreover, alternative and bent opal strips could also be fabricated using this protocol.[115] Yang produced chirped 3D photonic crystals in confined microchannels.[58] When a concentrated suspension of non-close-packed silica nanoparticles was applied to one side of the microchannels that prefilled with photocurable ethoxylated trimethylolpropane triacrylate (ETPTA) solution, the silica nanoparticles diffused and migrated to the distal ends to form a concentration gradient in the microchannel because of the force imbalance. Subsequent photopolymerization and removal of silica nanoparticles produced a chirped 3D photonic film with continuous changed lattice constant and color gradient, as shown in Figure 3c.

3.5.2 | Droplet confined assembly

Microfluidic technology also can offer a reliable and versatile route to the confined assembly of colloidal nanoparticles for optical purposes in a controlled fashion. Thanks to the precise and continuous manipulation of fluids at both geometrical and spatial levels, microdroplets and microcapsules with a variety of shapes (e.g., spherical, cylindrical, wire-like or tube-like shapes) containing the suspension of colloids can be expediently generated.[59,116,117] A subsequent solidification process produces photonic structures with morphologies in accord with the shapes of those microdroplets. It should be emphasized that the surfactant used for the stabilization of generated microdroplets together with other parameters including flow rates of liquid streams as well as density match between the inner and outer phases, play critical roles to manipulate the morphology of resultant photonic structures during the fabrication. Taking the spherical colloidal crystal beads for example, photonic beads with controllable sizes and narrow size distribution that displayed various distinct structural colors can be successively fabricated by a microfluidic device.[60,118–120] Colloidal suspension is sheared into monodisperse microdroplets in a continuous flow, and the subsequent evaporation of the solvent in the microdroplets drives the inner colloids to assemble into 3D periodic structures for color display. By using colloidal nanoparticles with different sizes as building blocks, microbeads with a variety of irradiate colors covering the entire visible region can be obtained. Using the microfluidic technique, double emulsion droplets with colloidal suspension encapsulated inside of polymer shells had been successfully fabricated.[61] The encapsulated colloidal nanoparticles gradually concentrated and self-assembled on the inner wall of the microcapsules after an extraction process. The resultant microbeads were composed of a transparent polymeric shell, a middle colloidal crystal layer, and an inner bubble core, which could serve as barcode particles. The number of encapsulated colloidal emulsion drops and the encoded elements could be modulated by varying the flow rates of the coflowing streams and the diameter of the colloidal nanoparticles, as shown in Figure 3d.

3.6 | Printing assisted assembly

3.6.1 | Ink-jet printing

The ink-jet printing technique developed in recent years has been considered as an efficient and versatile route to the fabrication of photonic crystals with complex patterns without using extra masks, templates, or selective etching process. The key to achieving this goal lies in the utilization of suspension containing monodisperse colloidal nanoparticles with desired sizes and surface properties as the printing ink. An ink-jet printing device typically includes an ink cartridge and an ink-jet head that can

accurately deposit the ink in a specific region of the substrate. During the printing process, the colloidal suspension has been directly sprayed onto a flexible or hard substrate by utilizing a commercial or customized ink-jet printer to form desired patterns. The evaporation of solvents and self-assembly of the colloidal nanoparticles eventually generate patterned photonic structures on demand. The printing resolution can be conveniently controlled by parameters including the nozzle diameter, evaporation behavior of the solvent, spray characteristics and viscosity of the ink. Due to its precise control of ink deposition and easy patterning, the ink-jet printing has gradually become a general method for the construction of photonic patterns. For example, by using latex suspensions containing core-shell nanoparticles with different sizes as the printing ink, macroscale patterned photonic crystals with multi-stopbands have been facilely obtained by ink-jet printing.[62] In addition, electrohydrodynamic jet printing that evolved from the ink-jet printing has been proposed to improve the printing resolution owing to its ability to generate uniform droplets or lines with sizes much smaller than the inner diameters of the nozzles.[63]

3.6.2 | 3D printing

Though ink-jet printing technique can achieve the facile fabrication of patterned photonic structures, the obtained structures are limited to planar shapes and geometries; therefore, it is still a great challenge to construct 3D photonic structures. To resolve this problem, 3D printing, which is recognized as a typical additive manufacturing technique, has emerged as a promising candidate to prepare multi-scale photonic structures with complex 3D geometries in a controlled fashion. Various strategies including direct ink writing (DIW),[121] direct laser writing (DLW),[64,122] and digital light processing (DLP)[123] have been developed to construct the 3D photonic structures via layer-by-layer stacking the building blocks from hydrogel, resin, or colloidal suspension-based printing inks. In a recent work reported by Hart and coworkers, they combined the colloidal self-assembly with direct-write 3D printing to fabricate macroscale free-standing colloidal structures. During the printing process, a liquid bridge was formed between the substrate and needle tip, which provided confinement for the assembly of colloidal nanoparticles at the base of the liquid bridge. The continuous moving of the substrate downward at the rate matched with the vertical growth rate of the assembled structure led to the formation of colloidal structures with high aspect ratio for photonic applications (Figure 4a).[65]

Two-photon polymerization lithography (TPL) has been considered as the typical DLW technique for the construction of 3D photonic structures. With its help, it is possible to directly produce photonic crystals with precise patterns in all three dimensions and realize a continuous hue of 3D photonic structure by controlling its lattice constants. Yang et al. introduced a heat-shrinking process into the TPL to obtain 3D printed photonic crystals with stopbands in the visible range.[64] As a result, woodpile photonic structures with vivid colors depending on their lattice constants had been generated (Figure 4b). With these woodpile photonic structures as color elements, 3D microscopic scale objects including a full-color 3D printed Eiffel Tower model with the height of 39 μm and a color pixel size of 1.45 μm was demonstrated for the first time. In addition, the 3D photonic structures can also be constructed by combining the bottom-up nanoparticle self-assembly with the top-down DLW technique. The exhibited coloration and photonic stopband can be controlled via the self-assembly of colloidal nanoparticles with desired sizes, while the geometrical 3D architectures can be manipulated with the assistance of ultraviolet or two-photon initiated polymerization of the hydrogel or resin that used as dispersion medium for the colloidal nanoparticles. Recently, we demonstrated that hydrogel-state or solid-state photonic microstructures with diverse compositions and free-designed 3D geometries could be achieved by using a degradable hydrogel as sacrificial scaffold to lock the self-assembled nanoparticles to minimize the disturbance effect of the femtosecond laser during the printing process, as shown in Figure 4c.[66] The minimum feature size of the resultant photonic microstructures could go down to 3 μm.

It should be mentioned that a DLP-based 3D printing technique has also been developed for the fabrication of 3D photonic structures in a layer-by-layer manner. Generally, the designed 3D structure is first sliced into layered images containing cross-sectional information. These images are continuously bottom-up projected for the crosslinking or polymerization of UV-curable structural color ink under the UV irradiation. As a result, the colloidal nanoparticles localized self-assemble within each cured layer to form non-close-packed ordered structures, which can further turn into close-packed structures after a subsequent evaporation induced shrinking process and endow the printed 3D structure volumetric color property. By utilizing the DLP 3D printing technique with hydrogen bond-assisted colloidal inks, various complex 3D structures with brilliant single or multi-structural colors were prepared, as shown in Figure 4d.[67]

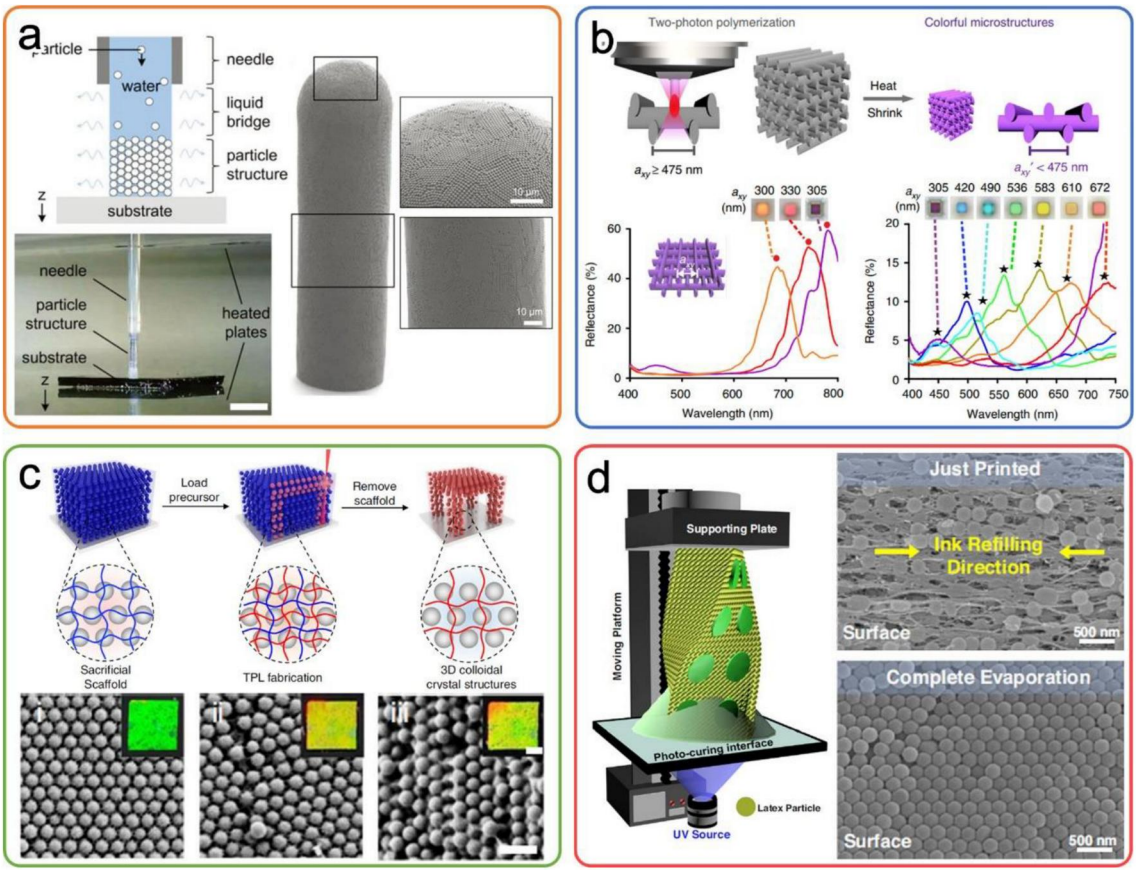

FIGURE 4 Photonic structures obtained by utilizing the printing technique: (a) macroscale free-standing colloidal structures fabricated by combining the colloidal self-assembly with direct-write 3D printing.[65] Copyright 2018 Wiley-VCH. (b) 3D printed woodpile photonic structures by using a heat-induced shrinking method.[64] Copyright 2019 Nature Publishing Group. (c) Photonic microstructures with diverse compositions and free-designed 3D geometries obtained by combining the bottom-up nanoparticle self-assembly with the top-down two-photon lithography.[66] Copyright 2022 Nature Publishing Group. (d) Complex 3D structures with single or multi-structural colors prepared by continuous DLP 3D printing.[67] Copyright 2022 Nature Publishing Group.

3.7 | Field induced assembly

3.7.1 | Electric field induced assembly

Since colloidal nanoparticles are nearly accompanied by certain surface charges, the assembly of charged nanoparticles can be conveniently manipulated by applying an external electric field, either alternating current (AC) field or direct current (DC) field. With the introduction of the electric field, charged monodisperse nanoparticles will be automatically attracted by the plane loaded with opposite charges and initiate the self-assembly due to the Coulomb interactions. The electric force exerted on the charged nanoparticles and the field-induced electrostatic interactions between neighboring nanoparticles can be precisely modulated by the applied electric field; thus, the electric field induced assembly of nanoparticles and the emerged optical properties of the resultant ordered structures are highly maneuverable.[124–127] Two typical examples using AC and DC fields to realize the controllable assembly of colloidal nanoparticles are presented, respectively. Velev and co-workers developed a novel electrically controlled chip for the fabrication of particles with advanced structures, in which controlled AC fields were applied through arrays of electrodes to hold and guide the droplets of various suspensions.[68] Since droplets were trapped above the area of highest field intensity where the dielectrophoretic force was strongest, they moved with the switching of the electrodes. Anisotropic "eyeball" supraparticles assembled via the evaporation of droplets from binary suspensions of gold nanoparticles and PS latex microspheres could be obtained using this technique. Solomon et al. utilized a low-voltage DC field to induce the self-assembly of colloidal nanoparticles with diverse sizes into close-packed ordered structures (Figure 5a).[69] Several different structural colors could be observed via the electronic field induced assembly by using colloids with different sizes, while a reversible change of the structural color from on to off could be switched by tuning the DC field on to off states.

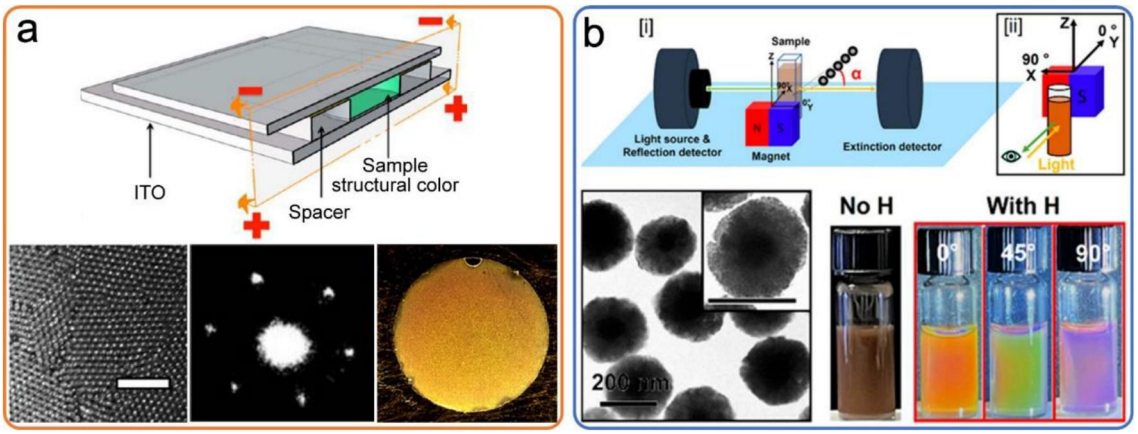

FIGURE 5 (a) The assembly of colloidal nanoparticles into close-packed ordered structures under a low-voltage DC field.[69] Copyright 2014 American Chemical Society. (b) The assembly of magnetoplasmonic colloidal nanoparticles under an external magnetic field.[70] Copyright 2023 American Chemical Society.

3.7.2 | Magnetic field induced assembly

The magnetic field induced assembly technique can be applied to nanoparticles with magnetic components for the fabrication of photonic structures. The magnetically active nanoparticles have the ability to rapidly respond to magnetic stimulus, thus it is highly feasible to realize the assembly of magnetic nanoparticles in a controlled fashion with the help of an external magnetic field. Both symmetric and asymmetric magnetic nanoparticles (e.g., spherical, ellipsoidal, spindle, or rod-shaped nanoparticles) can be used as building blocks for the establishment of ordered periodic structures for color exhibition.[128,129] For the spherical magnetic particles, it is well-known that they can organize into 1D chainlike structures when the repulsive and attractive forces maintain equilibrium in the presence of external magnetic field, thus diffraction of visible light and distinct structural color can be observed along the direction of magnetic field.[70,130] Moreover, magnetic nanoparticles doped with functional components such as plasmonic nanocrystals will result in novel tunable optical properties. For instance, magnetoplasmonic Ag@Fe_3O_4 core-shell nanoparticles can assemble into 1D photonic crystals with the help of external magnetic field to display angular-dependent and dynamically tunable colors, as shown in Figure 5b.[70] The combination of optical diffraction and plasmonic scattering enables programmable optical functionalities and precise modulation of the optical properties.

Unlike the spherical nanoparticles, the assembly of asymmetric magnetic nanoparticles such as ellipsoidal magnetic nanoparticles for color exhibition requires not only the spatial order but also the proper orientation of these nanoparticles due to their anisotropic morphologies. Tung and co-workers reported the fabrication of 3D periodic structures through oriented assembly of ellipsoidal γ-Fe_2O_3-SiO_2 core-shell nanoparticles in the presence of external magnetic field.[71] These nonspherical nanoparticles spontaneously oriented and aligned with their long axis parallel to the magnetic field. As a result, close-packed 3D ordered structures with different structural colors could be obtained by using ellipsoidal magnetic nanoparticles with different aspect ratios as building blocks. Further research revealed that the stop band of photonic structures assembled by the ellipsoidal magnetic nanoparticles could be well controlled by the direction of the applied magnetic field.[72]

4 | RESPONSIVE PHOTONIC CRYSTALS: CONTROL THE LIGHT PROPAGATION BY EXTERNAL STIMULI

In recent years, the demand for creating optical materials and devices with manipulatable optical properties is continuously increasing owing to their promising applications in sensors, bioassays, color displays and so on. Since the photonic crystal is capable of controlling the flow of light with the wavelength or frequency located in its photonic stop band, it has been considered as a competitive candidate for the fabrication of such photo-functional devices. According to the Bragg's Law, the photonic stop band and exhibited structural color are closely related to the average refractive index of the photonic crystals and the periodicity of the crystalline lattice. Therefore, they can be tuned by manipulating one or both of these two parameters. Materials such as liquid crystals, photochromic dyes, or polymers are usually infiltrated into the void of building blocks to modulate the average refractive index of the photonic crystals. On the other hand, stimulus-responsive materials including hydrogels, elastomers, or responsive nanocrystals are utilized to control the periodicity of the

spatial ordered structures. They are either directly used as dielectric building blocks for the construction of photonic crystals or used as a matrix for the immobilization of the dielectric building blocks. With the help of external stimuli, the introduction of functional components can realize the manipulation of the photonic stop band to control the light propagation and exhibit structural color. In this section, we will demonstrate the design, fabrication and application of photonic crystals with tunable photonic stop band, where external stimuli including temperature, mechanical stress, pH, ions, molecules, solvent, vapor, electric or magnetic field are utilized to modulate the refractive index and arrangement of dielectric building blocks to control their optical properties.

4.1 | Temperature responsive photonic crystals

Since some polymers such as poly(N-isopropylacrylamide) (PNIPAM) hydrogels and poly(oligo ethylene glycol acrylate) copolymers can undergo a reversible volume phase transition between a hydrated state and a dehydrated state upon the applied temperature, they have been widely utilized as thermosensitive components for the fabrication of responsive photonic crystals. To develop a thermochromic photonic structure, the monomer of thermosensitive gel is usually filled into the void of a close-packed colloidal crystal template and subsequently solidified under UV irradiation or thermal polymerization. Another choice is embedding the non-close-packed colloidal crystals in the matrix of thermosensitive polymers.[131–137] When increasing the temperature, the polymer matrix shrinks and the total volume decreases owing to the change in its hydrophilicity, eventually leading to the decrease of interparticle distance in the ordered structures, thus blue-shifting the reflection peak. On the contrary, when the temperature decreases, the swelling of the polymer matrix results in an opposite process. The reversible swelling and shrinking at a controlled temperature can effectively switch the diffraction of visible light. In a recent study reported by Zhang et al., a printing ink containing NIPAM and elastic colloidal nanoparticles was employed to fabricate the thermal-responsive 3D photonic patterns by utilizing the DLP 3D printing technique. During the printing process, colloidal nanoparticles were locked in the hydrogel matrix and assembled into non-closed-packed structures to display an obvious structural color. The thermosensitive PNIPAM hydrogel enabled a reversible volume change of the printed 3D photonic patterns when changing the temperature, leading to a corresponding change in the lattice distance and exhibited structural color, as shown in Figure 6a.[123] Moreover, the thermosensitive gel matrix with an inverse opal structure obtained by removal of the embedded colloidal nanoparticles also showed superior responsibility and sensibility. The tuning range of such gel matrix could cover the entire visible region.[141]

Besides the thermosensitive polymer gels, cholesteric liquid crystals (CLCs) also exhibit excellent thermochromic properties. Thanks to their helical structures, the periodic modulation of ordinary and extraordinary refractive indices along the helical axis helps the CLCs to yield a photonic stop band to selectively reflect visible light. The emerged photonic stop band is determined by the helical pitch, which is strongly influenced by the applied temperature. Thus, it can exhibit controlled structural color upon the applied temperature. Kim and co-workers successfully fabricated a novel kind of thermosensitive photonic capsules by encapsulating CLCs with a robust hydrogel poly(ethylene glycol) diacrylate (PEGDA) via a microfluidic approach.[142] The obtained microcapsules could freely suspend in water and serve as a colorimetric thermometer to provide temperature information of their surroundings over a wide volume. The microcapsules underwent a color change from green to red in the range of 20°C–88°C, confirming their good thermal sensitivity to the environmental temperature.

4.2 | Mechanical stress responsive photonic crystals

Mechanical stress has been considered as one kind of convenient and effective way to control the optical properties of photonic structures. In order to enable the mechanical deformation of photonic crystals without disturbing their periodical structures, robust elastic polymers are typically used as functional components for the construction of photonic structures, either directly used as dielectric building blocks or utilized to modify or embedding the building blocks.[143] Kolle and Vukusic reported a bio-inspired tunable elastic multilayer fiber, which was consisted of polydimethylsiloxane (PDMS) and polyisoprene-polystyrene triblock copolymer. These two elastomeric dielectrics initially formed a bilayer and then rolled up onto a thin glass fiber to generate the multilayer cladding.[144] Such multilayer hollow fiber could be elastically deformed by stretching along its axial direction. Such deformation would cause compression perpendicular to the elongation and a decrease in the thickness of each individual layer, eventually leading to a blue-shift of the reflection band. In this way, the exhibited color could be reversibly tuned. The band shift reached over 200 nm according to the elongation rate and original state. Hellmann and coworkers fabricated an

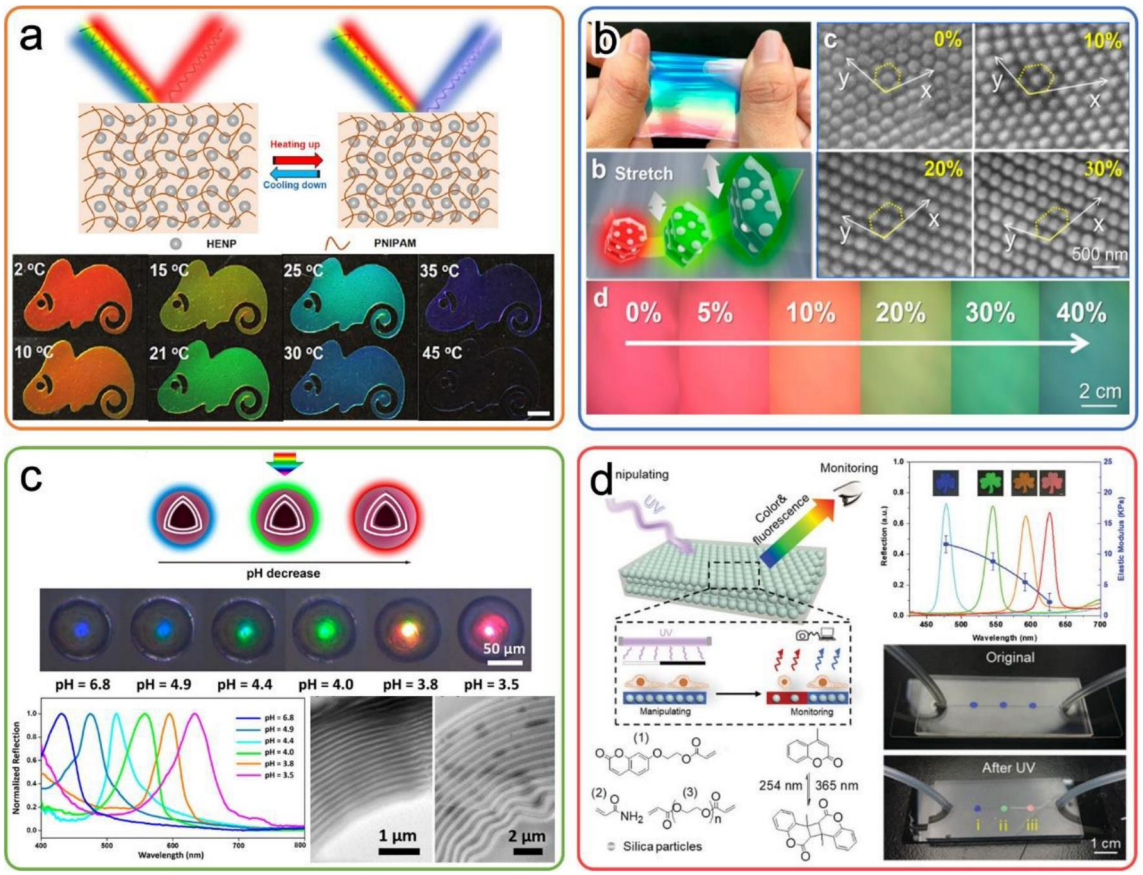

FIGURE 6 (a) Bio-inspired 3D-printed thermal-responsive chameleon patterned colloidal photonic crystals under different temperatures.[123] Copyright 2022 Elsevier Ltd. (b) An elastomeric opal film with reversible deformation capability obtained by embedding the ordered arrays of PS nanoparticles in the matrix of PEA elastomer via a shear-ordering process.[138] Copyright 2022 American Chemical Society. (c) pH-responsive photonic microcapsules formed by block copolymers via a self-emulsification strategy.[139] Copyright 2020 American Chemical Society. (d) A reconfigurable photonic hydrogel fabricated by embedding the silica nanoparticles in the hydrogel matrix containing coumarin derivatives.[140] Copyright 2020 Royal Society of Chemistry.

elastomeric opal film by using core-shell nanoparticles composed of rigid polystyrene-polymethyl methacrylate (PS-PMMA) core and soft deformable polyethyl acrylate shell as building blocks.[145,146] These core-shell nanoparticles were assembled through a melt-flow technique, afterward the resultant film was cross-linked by UV irradiation to gain the reversible deformability. Under the influence of external stain, the deformation in the colloidal lattice yielded a reversible change in the photonic stop band and the displayed color.

Infiltrating elastic monomer gels into the void of as-prepared photonic structures to overcome the inherent fragile characteristic, followed by a thermopolymerization or photopolymerization process for solidification is another strategy to achieve the mechanical stress-responsive photonic structures.[147–151] For instance, stretchable photonic films with reversibly color changes could be obtained by embedding the ordered array of colloidal nanoparticles in the matrix of polyethyl acrylate (PEA) elastomer. When the film was stretched, the film thickness decreased in the direction perpendicular to the stretching direction, leading to the extension of hexagonal (111) lattice plane and extrusion of lattice spacing in the perpendicular direction. Thus, a blue-shift in the reflection peak and exhibited structural color occurred, as shown in Figure 6b.[138] Gu and co-workers also utilized a similar strategy to obtain a tunable fiber Bragg grating by incorporating a stress-responsive colloidal crystal into the fiber.[152] By infiltrating the interparticle space of non-close-packed colloidal crystal array with an elastomeric polymer PEGDA, the elastomeric colloidal crystal array showed remarkable and reversible color change in response to applied mechanical stress. This phenomenon was attributed to the shrinkage or recover of PEGDA hydrogel, leading to the alteration of interparticle distance and the shift of photonic stop band. Hence, the optical properties of such elastic films could be easily modulated by the external mechanical stress in a controllable manner. The tuning range of the reflection peak was determined by the

stretching or compressing ratio and the volume fraction of polymer content.

4.3 | pH responsive photonic crystals

Hydrogel-based photonic sensors are of particular interest in recent years because they can be tailored to respond to a variety of stimuli including pH, ions, molecules, and temperature through a substantial volume phase transition that can manipulate the photonic stop band and light diffraction.[153] To construct a pH-responsive sensor, H^+ or OH^- sensitive functional groups are usually incorporated into the hydrogel matrix with photonic structures.[154,155] A pioneering work by Asher et al. developed an intelligent pH-responsive material by immobilizing highly charged monodisperse PS nanoparticles with non-close-packed ordered crystalline structures in a matrix of cross-linked polyacrylamide hydrogels. The hydrogel was further functionalized with two coupled recognition modules, a creatinine deiminase (CD) enzyme and a 2-nitrophenol (2NPh) titrating group, where the phenolate derivative 2NPh played a key role in response to the pH change.[156] These composite hydrogels underwent a reversible swelling or deswelling process in response to the pH stimulation. When the pH value was increased, deprotonation of the phenol groups caused the hydrogel to swell due to the increased solubility of the phenolate species. The volume phase transitions of the hydrogel led to changes in the interparticle distance and lattice constant of the ordered structures, hence changed the wavelength of diffracted light. Utilizing this mechanism, they have successfully realized the detection of creatinine in bodily fluids because the CD enzyme immobilized in the hydrogel could rapidly hydrolyze the analyte, while the released OH^- elevated the pH within the hydrogel and caused the swelling of hydrogels. Braun and Lee also developed a robust pH sensor through template assisted photo-polymerization of pH responsive hydrogel, 2-hydroxyethyl methacrylate (HEMA) and acrylic acid (AA) monomers within the void of a self-assembled photonic crystal.[157] The obtained hydrogel film with an inverse opal structure exhibited a rapid response to pH variations accompanied by a dramatic change in the film color, which derived from the swelling or collapse of the hydrogel due to the status change of carboxyl groups in the hydrogel.

In addition, the pH responsiveness can also be realized by photonic crystals formed by hydrogen ion-sensitive groups anchored polymers. Block copolymer has been recognized as another typical example to realize the construction of pH-responsive photonic crystals with controlled photonic stop band. Zhu et al. reported the fabrication of pH-responsive photonic microcapsules by using block copolymers via a self-emulsification strategy.[139] The block copolymers formed alternatingly stacked lamellar shell of the microcapsules after the solvent evaporation, which generated a bright structural color. The protonation of pyridine groups anchored on the lamellar shell in an acidic aqueous solution caused the selective swelling of block copolymers and the change of refractive index, leading to the shift of photonic stop band and exhibited structural color, as shown in Figure 6c.

4.4 | Light responsive photonic crystals

The optical properties of the photonic crystals can also be manipulated by light irradiation.[158–160] Liquid crystals (LCs) are one kind of the important functional materials for the construction of tunable photonic crystals with an optical response to light irradiation. They not only possess the ability to change the refractive index by manipulating their molecular orientation but also can control their optical properties through the phase transition. When the LCs are integrated with the photonic crystals, the molecular orientation of LCs such as 4-butyl-4-methoxyazobenzene can be readily controlled by UV-visible light irradiation.[161] These liquid crystal molecules go through a trans- to cis- photoisomerization under the irradiation of UV light, which can be recovered after visible light irradiation. The photoisomerization causes a phase transition of the LCs between the nematic phase and the isotropic phase. LCs align along the long axis of rod-like molecules in a nematic phase, which will turn into a disordered state in an isotropic phase. These two states can be reversibly switched by UV-visible light irradiation. Thus, it is possible to modulate the optical properties of the photonic crystals containing LCs.

Fluorescent dyes have been considered as another promising candidate to control the light propagation of the photonic crystals because they possess the ability to adsorb light with a certain wavelength for emission. When the frequency of adsorbed light or emitted light matches with the stop band of photonic crystals, the reflection intensity or even the wavelength of reflected light will be significantly changed. The fluorescent dyes can be directly loaded into the colloidal nanoparticles during the synthesis, or integrated with photonic crystals with the help of hydrogels such as polyacrylamide and PEGDA to enhance the tuning range and sensibility. Recently, a reconfigurable photonic hydrogel had been developed by copolymerizing coumarin-containing acrylate monomer and acrylic amide in the presence of monodispersed silica nanoparticles.[140] The embedded silica nanoparticles spontaneously assembled into ordered structures during the hydrogel formation to

generate structural color for the hybrid photonic hydrogel. It is worth noting that the coumarin derivatives in the hydrogel matrix underwent a dimerization or dedimerization process when they were illuminated by UV light with a specific wavelength. In this case, the crosslinking degree and stiffness of the hydrogel network were changed, leading to a swelling or shrinking of the hybrid hydrogel. Therefore, the change of interparticle distance among neighboring silica nanoparticles would cause the shift of photonic stop band and the alteration of exhibited structural color, as shown in Figure 6d.

4.5 | Ion and molecule responsive photonic crystals

As described above, polymer incorporated photonic crystal has been proved to be a versatile material for the fabrication of sensing devices for multitudinous purposes because it is quite convenient to endow functional groups or ligands to the photonic crystal via chemical modification or physical doping. When these functional groups or ligands interact with analytes such as ions and molecules, the bonding of analytes with photonic crystal would result in the change of average refractive index or even periodicity of the ordered structures. With the help of the active groups or ligands, it is not difficult to the control the photonic stop band and the exhibited structural color through the recognition of specific analytes.

Thomas et al. presented the dynamic swelling behavior of a block copolymer photonic lamellar gel with full-color tunability toward appropriate counteranions.[162] The polyelectrolyte block copolymer, polystyrene-b-poly(2-vinyl pyridine) (PS-b-P2VP) underwent changes in their chain dimension upon counteranion exchange, leading to selective swelling of the lamellar structures and switching of photonic stop band from transparent to various colors depending on the hydration characteristics of counteranions, as shown in Figure 7a. The recognition of different anions with well-controlled optical properties could also be achieved using photonic

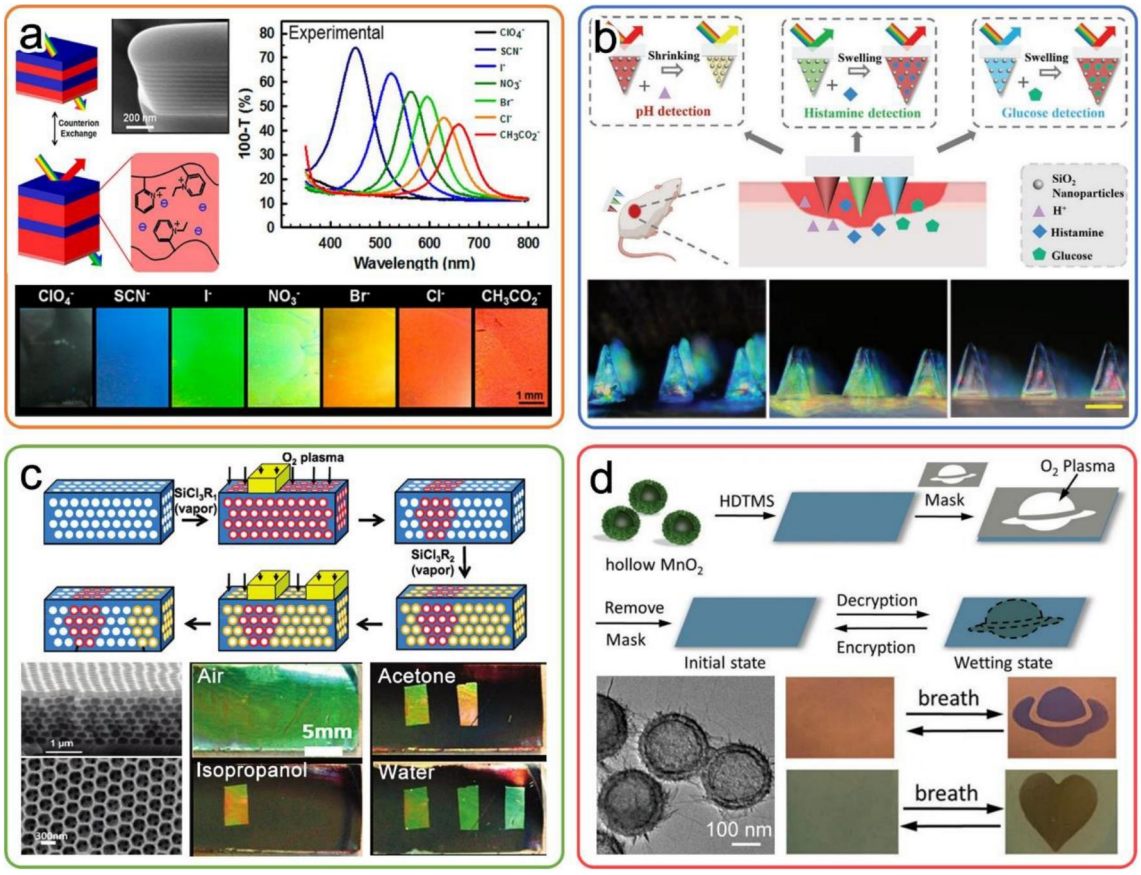

FIGURE 7 (a) A block copolymer photonic lamellar gel with full-color tunability in response to counteranions.[162] Copyright 2012 American Chemical Society. (b) Encoded photonic microneedle arrays for the detection of small molecules including histamine and glucose.[163] Copyright 2023 Wiley-VCH. (c) An inverse opal film with encoded wettability patterns.[164] Copyright 2011 American Chemical Society. (d) An encrypted film of hollow MnO_2 nanospheres that can reveal color information upon exposure to dynamic water vapor.[165] Copyright 2022 Wiley-VCH.

ionic liquid films,[166] polyelectrolyte films with inverse opal structures,[167] and inverse opal microspheres.[168] Besides the anions, sensing devices responsive to cations such as Na^+, K^+, Pb^{2+} and Hg^{2+} could be fabricated by utilizing the polymer-based photonic structures.[169,170] Our group developed an aptamer-functionalized photonic hydrogel film for the visual detection of heavy metal ions.[171,172] The cation-responsive aptamers were cross-linked in the hydrogel matrix containing an ordered colloidal crystal array of monodisperse silica nanoparticles. The specific binding of target cations with the aptamers in the hydrogel matrix caused the shrinkage of the hydrogel film. In this case, a corresponding blue-shift in the Bragg diffraction peak that relied on the concentration of cations could be recognized with naked eyes.

Asher is one of the pioneers to conduct research on the design and fabrication of responsive sensors that can effectively recognize specific molecules (e.g., the glucose in tear fluid) with different concentrations on the basis of a photonic crystal film composed of non-close-packed ordered crystalline structures in a matrix of responsive hydrogel.[173] When the target molecules interacted with the recognition elements in the hydrogel matrix, the hydrogels underwent a reversible swelling process depending on the molecule concentration. In this situation, the periodicity alteration in the crystal lattice shifted the photonic stop band and changed the displayed structural color. Further work had been conducted on improving the sensitivity and response speed of glucose at low concentration, thus it is possible to apply such responsive hydrogels to clinical diagnosis by integrating the hybrid hydrogels in a contact lens to monitor the approximate glucose levels of patients suffering from diabetes mellitus or hyperglycemia. Utilizing this mechanism, a biosensor on the basis of a responsive hydrogel for kinase detection has been developed.[174] This sensor showed reversible changes in optical properties from the ordered array of PS nanoparticles impregnated in the hydrogel upon the peptide phosphorylation and kinase activity. Another work reported by Zhao et al. demonstrated the fabrication of encoded photonic microneedle arrays for the detection of small molecules including histamine and glucose (Figure 7b).[163] Highly charged colloidal nanoparticles were integrated with the responsive hydrogels to construct the microneedle arrays with non-close-packed ordered structures in a microneedle mold. The sensing of histamine relied on the specific recognition of aptamers and target molecules, while the sensing of glucose was achieved by glucose-responsive fluorophenylboronic acid. When the microneedles interacted with these target molecules, the swelling or shrinking of the hybrid hydrogel caused a shift in the photonic stop band and change of the structural color.

4.6 | Solvent responsive photonic crystals

Taking advantage of a swelling and deswelling process, it has been proved that the periodicity of spatially ordered structures can also be effectively manipulated by certain solvent.[175–178] Xia's group developed a solvent responsive PDMS/PS colloidal crystal film by utilizing a swelling process.[179] When organic solvent was applied on the surface of the film with a patterned stamp, PDMS matrix in the area contact with the solvent pattern swelled, leading to the increase in interparticle distance and red-shift of the reflection peak. Therefore, a designed pattern with a color different from the background appeared. After the evaporation of the solvent, the PDMS matrix turned back to the original state and the color pattern would disappear. As a result, it is possible to reversibly control the photonic stop band by using solvents with diverse wettability or by controlling the swelling rate of the PDMS matrix. Yin also utilized a similar strategy to develop a rewritable photonic paper by embedding the Fe_3O_4@SiO_2 colloids in the PEGDA matrix.[180] Hygroscopic salt solution was used as ink to control the diffraction color patterns on the paper due to the swelling of the polymer matrix. Aizenberg demonstrated the fabrication of a solvent responsive inverse opal film with specific regioselective wetting patterns for different fluids.[164] A multistep vapor-functionalization and plasma-etching technique was utilized to generate complex wettability patterns on the multiple chemical functionalized film, including the exposure of entire film to vapors of alkylchlorosilanes for the modification of different functional groups to the inner surface of lattice structures, followed by masked plasma-etching to locally erase surface functionalities in the unpatterned region. The encoded patterns appeared optically invisible in dry status, while different pattern messages became visible when immerged the film into specific fluids such as isopropanol, acetone, and water due to the area-selective wetting of the functionalized patterns with controllable hydrophilicity and surface tension, as shown in Figure 7c. In this case, such a system could be used as a colorimetric sensor for a variety of liquids with diverse wettability.

4.7 | Vapor responsive photonic crystals

Photonic crystals have also been regarded as a promising material for the fabrication of sensors toward the detection of vapors in recent years since they exhibit strong ability to manipulate the photons and the flow of light. However, the innovation of advanced vapor sensitive photonic devices suffers a slow progress owing to inferior vapor adsorption

abilities of the lattice structures, thereby the selectivity and sensitivity of the photonic devices as well as the tuning range of the photonic stop band have been greatly restricted. To overcome this shortcoming, ordered periodical structures with higher porosity and larger specific surface area have been developed. For example, photonic structures assembled by using porous nanoparticles as building blocks, or photonic films with inverse opal structures obtained through the removal of particle templates can effectively improve their performance during the vapor sensing.[181–183] A patterned colloidal crystal array with multi-color shifting properties had been fabricated via ink-jet printing suspension of mesoporous silica nanoparticles as ink on various substrates.[184] These mesoporous silica nanoparticles enhanced the condensation process of vapor owing to the hierarchical porous structures, hence the change of refractive index was effectively improved. Core-shell mesoporous silica nanoparticles with diverse porosities or mesoporous shell thicknesses in different regions of the designed pattern presented diverse colors in the saturated ethanol vapor atmosphere, regardless of their identical structural color in a N_2 atmosphere. The difference in the change of refractive index of the mesopores was considered to be responsible for this phenomenon. Such dynamic vapor-chromic features of the responsive patterned film could be reversibly observed with naked eyes. On the basis of this mechanism, an optical nose chip was prepared by using surface-functionalized mesoporous silica beads for the detection of expiratory air of different people.[185] Yin et al. reported a color switching photonic film that fabricated by randomly assembled hollow manganese oxide (MnO_2) nanospheres for vapor sensing.[165] The color of the resultant film reversibly changed in response to dynamic water vapor, while no color shift was observed under static water vapor. This should be attributed to the filling of water in the mesoporous shells and inner cavities of the hollow MnO_2 nanospheres when exposed to dynamic water vapor, which would cause an obvious change in the refractive index and the exhibited color. Moreover, an encrypted film was obtained via selective hydrophobic modification. The color in the hydrophilic region dramatically changed while the hydrophobic region kept constant upon exposure to dynamic water vapor, as shown in Figure 7d.

4.8 | Electric field responsive photonic crystals

Since the electrostatic interactions are quite common among the charged colloidal nanoparticles and other building blocks for a photonic structure, thereby it is convenient and flexible to control the periodicity of such photonic structures with the help of an external electric field. Two strategies have been developed to achieve the color manipulation under an applied electric field, either by changing the lattice of the photonic structures via expansion/contraction of the dielectrics filling in the void of the colloidal nanoparticles or by electric field induced compression/relaxation of the building blocks.[186–188] To achieve this objective, tremendous effects have been devoted to the electrically tunable photonic materials during the past decades. One early attempt involved the imbibition of electrically tuned liquid crystals in the void of photonic structures.[161,189,190] However, only two colors that related to the phase transition of the liquid crystals between random and aligned states could be switched, which limited the optical tuning range and their potential applications. Ozin demonstrated the fabrication of electrically tunable photonic films by using the polyferrocenylsilane (PFS) derivatives as responsive component.[191] This kind of voltage-dependent photonic film was obtained by embedding the opal structures formed by silica nanoparticles in the matrix of PFS gel. When a potential more positive than the redox potential of the polymer was applied to such films, the PFS gel started to swell due to the influx of anions from the electrolyte and solvent into the polymer to compensate the extraction of electrons from the iron atoms in the polymer backbone, which caused the continuous red-shift of the diffraction peak. On the other hand, applying a reducing potential resulted in a reverse process. Therefore, reversible control of displayed structural color in almost the entire visible region had been realized with the help of an induced electronic field. Moreover, the subsequent removal of silica colloids to generate an inverse opal structure in the obtained film could effectively increase the tuning range, response rate, and decrease the driving voltage.[192,193]

Control the assembly of charged nanoparticles via compression or relaxation of the colloidal lattice with an external electric field is another route to the manipulation of photonic stop band. To achieve this goal, charged monodisperse nanoparticles with high refractive index (e.g., $ZnS@SiO_2$ nanoparticles, $Fe_3O_4@SiO_2$ nanoparticles, charged PS nanoparticles) have been utilized as building blocks for the photonic structures to achieve the fast and precise modulation of the photonic stop band in the visible region.[194–196] When an electric field is applied, the charged nanoparticles start to migrate and accumulate toward the oppositely charged electrode due to the electrostatic interactions. As a result, the photonic crystal lattice structure will be compressed on the side of the oppositely charged electrode, leading to manageable structural colors depending on the intensity of the electric field.[195] It is worth mentioning that once the charged nanoparticles are compressed to show structural colors

different from their initial state, the electric field has to be maintained to balance the electrophoretic packing force and electrostatic repulsion force to keep the color stable. Recently, an electrically responsive photonic crystal with bistable states and switchable characteristics had been developed by introducing polyethylene glycol (PEG) in the electrophoretic ink containing monodisperse silica nanoparticles. Such responsive photonic crystal had two stable states at 0 V, including the colored state from colloidal self-assembly that could be reversibly switched by applying an electric field, and colorless state with disordered particle arrangement, as shown in Figure 8a.[197]

4.9 | Magnetic field responsive photonic crystals

Endowing photonic crystals with magnetic properties has emerged as another efficient strategy to control the periodicity and photonic stop band of constructed ordered structures. In recent years, magnetic colloidal nanoparticles have demonstrated themselves as promising candidates in the fabrication of photonic structures with tunable optical properties. The magnetic colloidal nanoparticles can assemble into ordered structures in the presence of external magnetic field. Without the magnetic stimulus, the magnetic colloidal nanoparticles randomly suspend in the solutions due to the Brownian motion as well as the interparticle repulsive force from macromolecular steric hindrance or charged groups bonding on the surface of the nanoparticles. Thanks to the rapid responsiveness of the magnetic colloidal nanoparticles, non-close-packed chainlike ordered structures parallel to the direction of the magnetic field will be formed in solutions after applying an external magnetic field. In the direction perpendicular to that of the magnetic field, the magnetic colloidal nanoparticles are affected by interparticle repulsive force and magnetic repulsive force between magnetic dipoles, which keep them away from each other to prevent immediate aggregation. Meanwhile, in the direction parallel to that of the magnetic field, they are mainly affected by the interparticle repulsive force and magnetic attractive force. The balance between the attractive and repulsive force will form in the condition that the intensity of the magnetic field is strong enough, leading to a temporary stabilization of neighboring nanoparticles with a certain interparticle distance to diffract visible light and exhibit distinct structural color.[199–202] By manipulating the intensity of the applied magnetic field, it is possible to control the interparticle distance and periodicity of the formed ordered structures to achieve the exhibition of variable structural colors. The key to achieving the controlled diffraction of visible light relies on uniform superparamagnetic colloidal nanoparticles with a certain diameter and narrow size distribution that are dispersed in solution or a solution-like environment, either spherical aggregations with certain sizes directly formed by magnetic clusters,[203–205] or composite nanoparticles with core-shell[206] or randomly dispersed structures.[198,207]

Yin et al. developed a high temperature hydrolysis process for the synthesis of superparamagnetic colloidal crystal clusters with the tuning range covering the entire visible region when induced by an external magnetic field.[203] Because these magnetic clusters were constituted only by magnetite that stabilized by a surface layer of polyacrylic acid, they had extremely high magnetic content and saturated magnetization. With the assistance of a magnetic stimulation, they could self-assemble into ordered lattices to diffract visible light with different

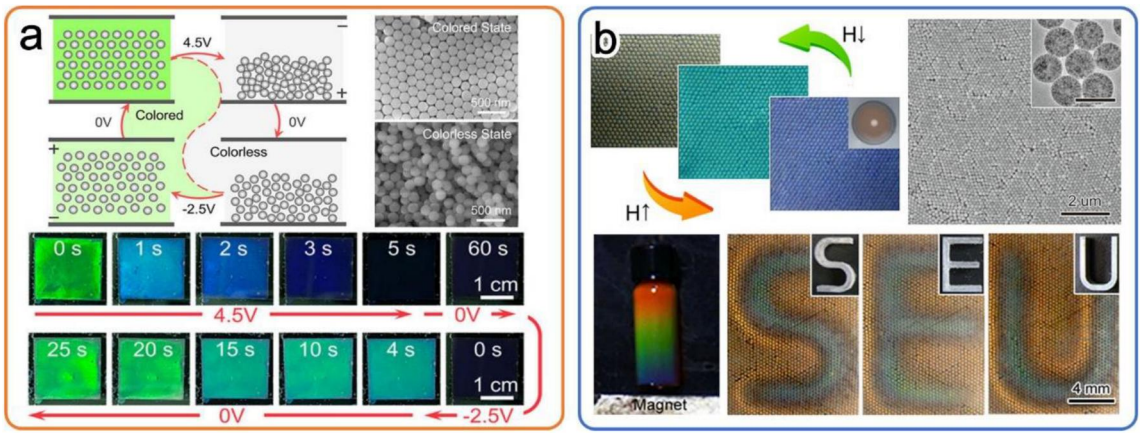

FIGURE 8 (a) Electrically responsive photonic crystals with bistable states at 0 V and switchable structural colors obtained by introducing PEG in the electrophoretic ink.[197] Copyright 2022 Nature Publishing Group. (b) A magnetochromatic microcapsule array for dynamic color display in the presence of a tunable magnetic field.[198] Copyright 2011 Wiley-VCH.

wavelengths according to the distance between the magnet and the sample, thus the magnetic intensity acting on these clusters. Philipse's group reported the fabrication of a core-shell type monodisperse magnetic polymethyl methacrylate (PMMA) spheres that exhibited field-induced colloidal crystallization. Under a gradient magnetic field, the resultant magnetic crystals presented iridescent structural colors due to the inhomogeneous field gradient offered by the magnet, which was used to induce the arrangement and periodicity of the magnetic colloidal crystals.[206] Gu and coworkers utilized a modified mini-emulsion polymerization to fabricate the monodisperse Fe_3O_4/PS composite superparamagnetic nanoparticles. A great deal of Fe_3O_4 nanocrystals were randomly incorporated into the composite nanoparticles during the synthesis, giving rapid magnetic responsiveness to the resultant composite nanoparticles.[198,207] Such nanoparticles also had the ability to assemble into a periodic structure for light diffraction and color exhibition, with a tuning range covering the whole visible spectrum (Figure 8b).

The real-time and reversible magnetic field responsive properties of the magnetic nanoparticles successfully make them ideal candidates for the design of futuristic functional optical devices such as microcarriers, bioassays, sensors, or color displays. Since the magnetic nanoparticles tend to align along the direction of external magnetic field, strong irradiate color can be observed in the direction parallel to the magnetic field. Such color will immediately disappear when removing the magnetic field. Thus, the emerged structural color has been endowed with "on" and "off" two different states. Moreover, contactless control of the structural color on designed pixels can be realized owing to the remote induction of the magnetic nanoparticles toward the external magnetic field, which is beneficial for the fabrication of flexible devices. Kwon demonstrated the high-resolution patterning of multiple structural colors on the basis of a maskless lithography system.[208] A mixture composed of superparamagnetic Fe_3O_4@SiO_2 colloids, a solvation liquid, and a photocurable resin was served as the M-ink, whose color could be conveniently modulated by an external magnetic field with controlled intensity. When the desired color for a specific pattern was achieved under a certain magnetic field intensity, the UV light was applied to fix the ordered chainlike structures of the superparamagnetic particles in the M-ink with the help of a computer-controlled spatial light modulator as mask. Taking advantage of such technique, a variety of free-floating barcodes with different colors and patterns for multiplex high-throughput bioassays had been fabricated by simply changing the induced mask and the magnetic field intensity.[209] Yin developed a display device by patterning a mixture of PDMS and Fe_3O_4@SiO_2 colloids dispersed ethylene glycol (EG) droplets.[210] Two kinds of Fe_3O_4@SiO_2 core-shell colloids with the same core diameter but different shell thicknesses were filled into the letter patterns and background of the film, respectively. The resultant film could switch its color from natural brown to desired colors after applying a magnetic field; thus, the specific color pattern could be displayed according to the colloid size and the strength of the external magnetic field. Our group also presented a magnetochromatic microcapsule array to achieve the dynamic color display.[198] Each microcapsule in the array could be considered as an individual display unit, whose shell was formed by transparent photocurable ethoxylated trimethylolpropane triacrylate (ETPTA) resin while the core was composed of an aqueous droplet containing monodisperse magnetic nanoparticles. The nanoparticles in the core droplet maintained the ability to rapidly and reversibly respond to the external magnetic field and assemble into ordered structures for light diffraction; therefore, various distinct colors could be exhibited according to the field intensity.

4.10 | Multiple stimuli responsive photonic crystals

Though a wide variety of photonic crystals that possess tunable periodic structures and structural colors have been reported, most of them can only respond to single specific stimulus, which is not favorable for the fabrication of futuristic sensing devices working in a complex environment for diverse purposes. The fabrication of photonic sensing devices with superior performance that possess the ability to respond to multiple stimuli is still a challenge owing to the relatively complex manufacturing process, high cost, as well as the lack of reliable mechanism and technique. Hence, it is essential to develop tough photonic systems containing multifunctional components with diverse levels of tunability and responsibility toward multiple external stimuli to open a new avenue for practical applications.

Some research work in regard to multi-responsive photonic systems has been demonstrated to achieve this objective in recent years.[211–216] For example, a multiple stimuli-responsive photonic hydrogel with a lamellar structure consisting of hard poly(dodecylglyceryl itaconate) (PDGI) bilayers periodically stacked in the interpenetrating soft layers composed of poly(acrylamide) (PAAm) and poly(acrylic acid) (PAAc) had been proposed. The photonic stop band of such hydrogel could be reversibly switched in response to various

external stimuli including temperature, pH, and mechanical stress with a wide tuning range.[217] The reversible association and dissociation of hydrogen bonds between PAAm and PAAc in the soft layer as well as the dissociation of carboxy group of PAAc at high pH played a key role in thermo- and pH-chromatic behavior, respectively. In addition, the photonic hydrogel was also responsive to mechanical stress by controlling the periodicity of the alternative stacks (Figure 9a). Gallei et al. reported a robust triple-responsive elastomeric opal film obtained via extrusion and compression molding of core-shell colloidal nanoparticles.[219] Taking advantage of the soft shell composed of ethyl acrylate (EA), iso-butyl methacrylate (IBMA), and HEMA in the building blocks, the resultant film exhibited fully reversible mechano-chromatic behavior. Distinct blue-shift in transmission spectra and apparent color change of the flexible opal film could be observed upon film elongation. The color switch was attributed to the decrease of the spacing in the (111) plane under the influence of a small stain, followed by a transition of the lattice from an ordered (111) state to a reorganized (200) state when sequentially increasing the strain. The incorporation of a temperature sensitive and polymerizable rhodamine B derivative either in the core or in the shell of these nanoparticles during the stepwise emulsion polymerization also endowed the light and temperature responsiveness to the obtained elastomeric opal film. The reversible transition between the open and closed forms of the fluorochrome rhodamine B derivative embedded in the nanoparticles under the UV irradiation or high temperature resulted in the display and erase of the patterned photoactivated information, indicating that the resultant film was stimulable by multiple triggers including mechanical stress, light, and temperature. Our group also fabricated multiresponsive structural color patterns by using monodisperse elastic poly(methyl methacrylate-butyl acrylate) (P(MMA-BA)) copolymer nanoparticles with controlled sizes as building blocks. Taking advantage of the relatively low glass transition temperature of the copolymer nanoparticles, the mechanical and optical properties of the assembled photonic structures had been remarkably enhanced. The resultant elastic photonic film not only could conceal or exhibit the encrypted color information but also could rapidly and reversibly respond to external stimuli including the solvent, pH, and tensile force, as shown in Figure 9b.[218]

Despite the performance, it is not difficult to obtain photonic crystals possessing the ability to respond to multiple stimuli. However, achieving an independent and spatially controlled response in the multiresponsive photonic crystals is quite important and essential because it allows more degree of freedom for practical applications in complex environments. Recently, a stretchable chromotropic ionic skin that possessed the ability to simultaneously detect and decouple multiple stimuli including strain, temperature, and pressure had been reported by Kim and coworkers.[211] The mechanochromic, thermoresistive, and triboelectric sensing were realized by means of the strain-sensitive color switching from the array of Fe_3O_4@C core-shell nanoparticles with a mechanochromic photonic crystal structure, temperature-sensitive resistance from the thermoresistive effect of temperature-sensitive ionic hydrogel, and pressure-sensitive voltage signal from a wrinkle-patterned PDMS film with gradient modulus and carbon nanotubes based electrode, respectively (Figure 9c).

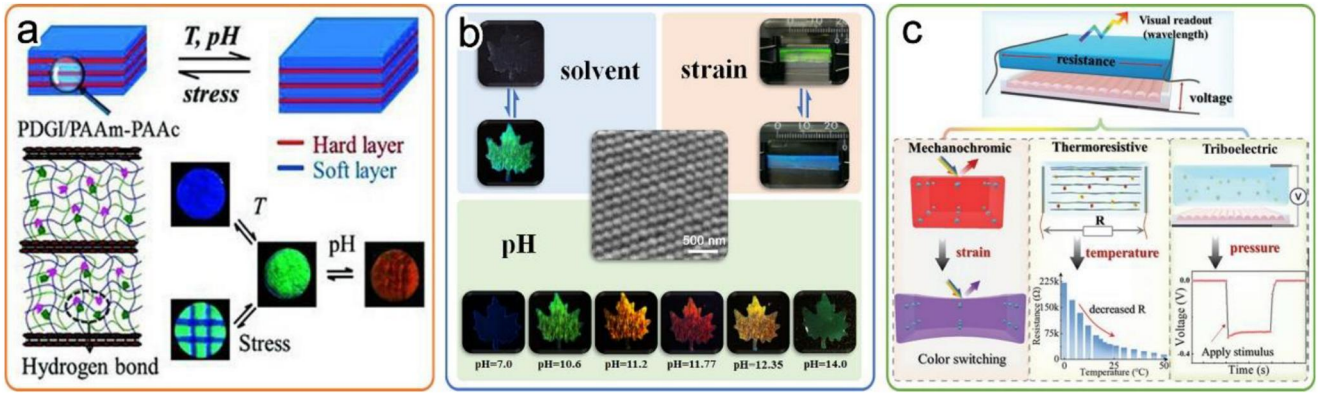

FIGURE 9 (a) A photonic hydrogel with reversible responsiveness to various external stimuli including temperature, pH, and mechanical stress.[217] Copyright 2013 Wiley-VCH. (b) Multiresponsive structural color patterns that can rapidly and reversibly respond to solvent, pH, and tensile force.[218] Copyright 2019 Wiley-VCH. (c) A stretchable chromotropic ionic skin that can simultaneously detect and decouple multiple stimuli including strain, temperature, and pressure.[211] Copyright 2022 Wiley-VCH.

5 | SUMMARY AND OUTLOOK

In this review, we have summarized recent developments in bio-inspired photonic crystals regarding the design and manipulation of dielectric building blocks into spatially ordered structures with diverse dimensions for selective light diffraction. On the basis of mechanisms inspired from nature for the exhibition of vivid iridescent color, considerable photonic materials and devices have been developed with the objective to modulate the flow of light in a controlled fashion. Besides the fabrication of photonic crystals with static colors, strategies for modulating the photonic stop band in the presence of external stimuli to achieve the control of light propagation have been outlined in this review. Due to the unique optical properties provided by photonic crystals, they have been widely applied to multitudinous areas such as waveguides, anti-counterfeiting, security, bioassays, sensors and optical devices.

Although we have enjoyed the convenience brought by photonic crystals, lots of efforts still need to be devoted to the fabrication of high-quality photonic crystals. Since the optical properties of photonic crystals are determined by the arrangement of dielectric building blocks and the refractive index, even small diversity in scale, structure, or morphology of the building blocks may result in massive changes in the physicochemical properties. Take the colloidal nanoparticles for example, though monodisperse colloids have the ability to self-assemble into 3D photonic crystals, a large number of intrinsic defects such as cracks and lattice mismatch is quite common and usually accompanied by the assembled spatial ordered structures because of the small diversity in size of the colloids. This will reduce their mechanical strength and efficiency for the selective diffraction of light. Despite the use of well-defined defects in photonic crystals for optical applications (e.g., waveguides, switches, laser devices), it remains a challenge to fabricate photonic crystals free of defects in large scales up to date owing to the intrinsic defects, time-consuming assembly process, and relatively high cost. Hence, it is critical to develop novel techniques to reduce the preparation cost, accelerate the assembly and simplify the fabrication process to obtain photonic crystals with higher quality in large scale so as to expand their applications beyond laboratory level. For example, achieving a novel emulsification technique to generate uniform emulsified microdroplets will be beneficial for the synthesis of monodisperse colloidal nanoparticles for photonic crystals. Moreover, the symmetries or structures of photonic crystals are greatly affected by packing forces such as van der Waals force, gravity force, and capillary force during the colloidal assembly. However, it is still a critical challenge to precisely describe and control these forces. The utilization of recently developed artificial intelligence (AI) technology for simulation and calculation may open a new avenue to solve this problem and provide guidance for the fabrication of photonic crystals with higher quality.

Embedding the spatially ordered structures in the responsive polymer matrix or incorporating responsive components with the building blocks can effectively endow the photonic crystals with stimuli responsiveness. Responsive polymers such as hydrogels, elastomers, and field-responsive molecules or nanocrystals are frequently used as functional components to construct the responsive photonic crystals. It should be pointed out that currently most sensing devices on the basis of responsive photonic crystals almost suffer from problems such as irreversible changes in the ordered structures after single use, relatively small changes and tuning range of optical signal, or long response time required toward the stimulus. To apply the responsive photonic crystals to practical applications, we need to pay special attention to the stability, tuning range, response time, and reversibility of the constructed photonic sensors. The transition speed of the spatially ordered structures should be fast enough to ensure a short responsive time, which means real-time responsive and dynamic tunable optical properties need to be achieved. In addition, the precise control of the optical signal cross the visible region together with an obvious color change toward a small stimulus that can be recognized with naked eyes should also be taken into consideration. Strategies such as developing novel sensing materials and modifying the building blocks with highly efficient functional groups or ligands may improve the stability, sensitivity and repeatability of the responsive photonic crystals. Hence, it is not only a challenge but also an opportunity for us. In our opinion, with the development of advanced technology, the bio-inspired photonic crystals will encounter a much brighter future in both theoretical development and practical application, which will effectively promote the interdisciplinary cooperation and bring more convenience to our daily life.

ACKNOWLEDGMENTS

This work is financially supported by the Natural Science Foundation of Jiangsu Province (BK20202013), the National Key R&D Program of China (No. 2017YFA0700500), and the 111 Project (B17011).

CONFLICT OF INTEREST STATEMENT

Zhongze Gu is an editorial board member of this journal and was not involved in the editorial review or the decision to publish this article. All authors declare that there are no conflicts of interest.

ORCID

Cun Zhu https://orcid.org/0000-0003-3764-4523

REFERENCES

1. E. Yablonovitch, *Phys. Rev. Lett.* **1987**, *58*, 2059.
2. S. John, *Phys. Rev. Lett.* **1987**, *58*, 2486.
3. B. Gates, Y. Xia, *Adv. Mater.* **2001**, *13*, 1605.
4. S. Y. Choi, M. Mamak, G. von Freymann, N. Chopra, G. A. Ozin, *Nano Lett.* **2006**, *6*, 2456.
5. Y. Takeoka, M. Honda, T. Seki, M. Ishii, H. Nakamura, *ACS Appl. Mater. Interfaces* **2009**, *1*, 982.
6. K. Ueno, Y. Sano, A. Inaba, M. Kondoh, M. Watanabe, *J. Phys. Chem. B* **2010**, *114*, 13095.
7. H. Gu, Y. Zhao, Y. Cheng, Z. Xie, F. Rong, J. Li, B. Wang, D. Fu, Z. Gu, *Small* **2013**, *9*, 2266.
8. Z. Li, Q. Fan, Y. Yin, *Chem. Rev.* **2022**, *122*, 4976.
9. Z. Cai, Z. Li, S. Ravaine, M. He, Y. Song, Y. Yin, H. Zheng, J. Teng, A. Zhang, *Chem. Soc. Rev.* **2021**, *50*, 5898.
10. P. Wu, J. Wang, L. Jiang, *Mater. Horiz.* **2020**, *7*, 338.
11. J. Hou, M. Li, Y. Song, *Nano Today* **2018**, *22*, 132.
12. G. Isapour, M. Lattuada, *Adv. Mater.* **2018**, *30*, 1707069.
13. S. Tadepalli, J. M. Slocik, M. K. Gupta, R. R. Naik, S. Singamaneni, *Chem. Rev.* **2017**, *117*, 12705.
14. N. Vogel, M. Retsch, C.-A. Fustin, A. Campo, U. Jonas, *Chem. Rev.* **2015**, *115*, 6265.
15. C. Fenzl, T. Hirsch, O. S. Wolfbeis, *Angew. Chem., Int. Ed.* **2014**, *53*, 3318.
16. N. Zhao, Z. Wang, C. Cai, H. Shen, F. Liang, D. Wang, C. Wang, T. Zhu, J. Guo, Y. Wang, X. Liu, C. Duan, H. Wang, Y. Mao, X. Jia, H. Dong, X. Zhang, J. Xu, *Adv. Mater.* **2014**, *26*, 6994.
17. M. Maldovan, *Nature* **2013**, *503*, 209.
18. G. von Freymann, V. Kitaev, B. V. Lotsch, G. A. Ozin, *Chem. Soc. Rev.* **2013**, *42*, 2528.
19. A. Stein, B. E. Wilson, S. G. Rudisill, *Chem. Soc. Rev.* **2013**, *42*, 2763.
20. J. Ge, Y. Yin, *Angew. Chem., Int. Ed.* **2011**, *50*, 1492.
21. F. Marlow, Muldarisnur, P. Sharifi, R. Brinkmann, C. Mendive, *Angew. Chem., Int. Ed.* **2009**, *48*, 6212.
22. S. Kinoshita, S. Yoshioka, J. Miyazaki, *Rep. Prog. Phys.* **2008**, *71*, 076401.
23. A. R. Parker, *J. Opt. A: Pure Appl. Opt.* **2000**, *2*, R15.
24. A. R. Parker, N. Martini, *Opt. Laser Technol.* **2006**, *38*, 315.
25. J. P. Vigneron, P. Simonis, *Physica B* **2012**, *407*, 4032.
26. M. R. Weatherspoon, Y. Cai, M. Crne, M. Srinivasarao, K. H. Sandhage, *Angew. Chem., Int. Ed.* **2008**, *47*, 7921.
27. R. C. McPhedran, N. A. Nicorovici, D. R. McKenzie, G. W. Rouse, L. C. Botten, V. Welch, A. R. Parker, M. Wohlgennant, V. Vardeny, *Physica B* **2003**, *338*, 182.
28. J. Teyssier, S. V. Saenko, D. van der Marel, M. C. Milinkovitch, *Nat. Comm.* **2015**, *6*, 6368.
29. H. Cong, B. Yu, X. S. Zhao, *Opt. Exp.* **2011**, *19*, 12799.
30. J. P. Vigneron, J. M. Pasteels, D. M. Windsor, Z. Vértesy, M. Rassart, T. Seldrum, J. Dumont, O. Deparis, V. Lousse, L. P. Biró, D. Ertz, V. Welch, *Phys. Rev. E* **2007**, *76*, 031907.
31. S. Kinoshita, S. Yoshioka, *ChemPhysChem* **2005**, *6*, 1442.
32. A. R. Parker, *Philos. Trans. R. Soc., A* **2004**, *362*, 2709.
33. S. Vignolini, P. J. Rudall, A. V. Rowland, A. Reed, E. Moyroud, R. B. Faden, J. J. Baumberg, B. J. Glover, U. Steiner, *Proc. Natl. Acad. Sci. U. S. A.* **2012**, *109*, 15712.
34. R. A. Potyrailo, H. Ghiradella, A. Vertiatchikh, K. Dovidenko, J. R. Cournoyer, E. Olson, *Nat. Photonics* **2007**, *1*, 123.
35. S. Yoshioka, S. Kinoshita, *Proc. R. Soc. B* **2006**, *273*, 129.
36. H. M. Whitney, M. Kolle, P. Andrew, L. Chittka, U. Steiner, B. J. Glover, *Science* **2009**, *323*, 130.
37. J. Zi, X. Yu, Y. Li, X. Hu, C. Xu, X. Wang, X. Liu, R. Fu, *Proc. Natl. Acad. Sci. U. S. A.* **2003**, *100*, 12576.
38. B. D. Wilts, K. Michielsen, H. D. Raedt, D. G. Stavenga, *Interface Focus* **2012**, *2*, 681.
39. P. Vukusic, J. R. Sambles, *Nature* **2003**, *424*, 852.
40. S. Yoshioka, H. Fujita, S. Kinoshita, B. Matsuhana, *J. R Soc. Interface* **2014**, *11*, 20131029.
41. P. Simonis, J. P. Vigneron, *Phys. Rev. E* **2011**, *83*, 011908.
42. V. Welch, V. Lousse, O. Deparis, A. Parker, J. P. Vigneron, *Phys. Rev. E* **2007**, *75*, 041919.
43. Q. He, K. H. Ku, H. Vijayamohanan, B. J. Kim, T. M. Swager, *J. Am. Chem. Soc.* **2020**, *142*, 10424.
44. Q. Guo, R. Xue, J. Zhao, Y. Zhang, G. T. van de Kerkhof, K. Zhang, Y. Li, S. Vignolini, D.-P. Song, *Angew. Chem., Int. Ed.* **2022**, *61*, e202206723.
45. X. Chen, H. Mayama, G. Matsuo, T. Torimoto, B. Ohtani, K. Tsujii, *J. Colloid Interface Sci.* **2007**, *305*, 308.
46. Y. Wang, M. Li, E. Colusso, W. Li, F. G. Omenetto, *Adv. Opt. Mater.* **2018**, *6*, 1800066.
47. O. Sanchez-Sobrado, M. E. Calvo, H. Mıguez, *J. Mater. Chem.* **2010**, *20*, 8240.
48. L. Passoni, L. Criante, F. Fumagalli, F. Scotognella, G. Lanzani, F. D. Fonzo, *ACS Nano* **2014**, *8*, 12167.
49. J.-T. Zhang, L. Wang, D. N. Lamont, S. S. Velankar, S. A. Asher, *Angew. Chem., Int. Ed.* **2012**, *51*, 6117.
50. J.-T. Zhang, X. Chao, S. A. Asher, *J. Am. Chem. Soc.* **2013**, *135*, 11397.
51. H. Fudouzi, *J. Colloid Interface Sci.* **2004**, *275*, 277.
52. C.-H. Hsieh, Y.-C. Lu, H. Yang, *ACS Appl. Mater. Interfaces* **2020**, *12*, 36478.
53. M. Bitsch, A. K. Boehm, A. Grandjean, G. Jung, M. Gallei, *Molecules* **2021**, *26*, 7350.
54. K. R. Phillips, T. Shirman, E. Shirman, A. V. Shneidman, T. M. Kay, J. Aizenberg, *Adv. Mater.* **2018**, *30*, 1706329.
55. Z.-Z. Gu, A. Fujishima, O. Sato, *Chem. Mater.* **2002**, *14*, 760.
56. S. H. Park, D. Qin, Y. Xia, *Adv. Mater.* **1998**, *10*, 1028.
57. Y. Yin, Y. Lu, B. Gates, Y. Xia, *J. Am. Chem. Soc.* **2001**, *123*, 8718.
58. S.-H. Kim, W. C. Jeong, H. Hwang, S.-M. Yang, *Angew. Chem., Int. Ed.* **2011**, *50*, 11649.
59. T. Kanai, D. Lee, H. C. Shum, R. K. Shah, D. A. Weitz, *Adv. Mater.* **2010**, *22*, 4998.
60. S.-H. Kim, S.-J. Jeon, S.-M. Yang, *J. Am. Chem. Soc.* **2008**, *130*, 6040.
61. L. Shang, F. Fu, Y. Cheng, H. Wang, Y. Liu, Y. Zhao, Z. Gu, *J. Am. Chem. Soc.* **2015**, *137*, 15533.
62. L. Cui, Y. Li, J. Wang, E. Tian, X. Zhang, Y. Zhang, Y. Song, L. Jiang, *J. Mater. Chem.* **2009**, *19*, 5499.
63. H. Ding, C. Zhu, L. Tian, C. Liu, G. Fu, L. Shang, Z. Gu, *ACS Appl. Mater. Interfaces* **2017**, *9*, 11933.
64. Y. Liu, H. Wang, J. Ho, R. C. Ng, R. J. H. Ng, V. H. Hall-Chen, E. H. H. Koay, Z. Dong, H. Liu, C.-W. Qiu, J. R. Greer, J. K. W. Yang, *Nat. Comm.* **2019**, *10*, 4340.
65. A. T. L. Tan, J. Beroz, M. Kolle, A. J. Hart, *Adv. Mater.* **2018**, *30*, 1803620.

66. K. Liu, H. Ding, S. Li, Y. Niu, Y. Zeng, J. Zhang, X. Du, Z. Gu, *Nat. Commun.* **2022**, *13*, 4563.
67. Y. Zhang, L. Zhang, C. Zhang, J. Wang, J. Liu, C. Ye, Z. Dong, L. Wu, Y. Song, *Nat. Commun.* **2022**, *13*, 7095.
68. J. R. Millman, K. H. Bhatt, B. G. Prevo, O. D. Velev, *Nat. Mater.* **2005**, *4*, 98.
69. A. A. Shah, M. Ganesan, J. Jocz, M. J. Solomon, *ACS Nano* **2014**, *8*, 8095.
70. C. Wu, Q. Fan, W. Wu, T. Liang, Y. Liu, H. Yu, Y. Yin, *Nano Lett.* **2023**, *23*, 1981.
71. T. Ding, K. Song, K. Clays, C.-H. Tung, *Adv. Mater.* **2009**, *21*, 1936.
72. M. Wang, L. He, W. Xu, X. Wang, Y. Yin, *Angew. Chem., Int. Ed.* **2015**, *54*, 7077.
73. S. Guldin, M. Kolle, M. Stefik, R. Langford, D. Eder, U. Wiesner, U. Steiner, *Adv. Mater.* **2011**, *23*, 3664.
74. G. M. Miyake, R. A. Weitekamp, V. A. Piunova, R. H. Grubbs, *J. Am. Chem. Soc.* **2012**, *134*, 14249.
75. D. J. Mulder, A. P. H. J. Schenning, C. W. M. Bastiaansen, *J. Mater. Chem. C* **2014**, *2*, 6695.
76. H. Eoh, Y. Jung, C. Park, C. E. Lee, T. H. Park, H. S. Kang, S. Jeon, D. Y. Ryu, J. Huh, C. Park, *Adv. Funct. Mater.* **2022**, *32*, 2103697.
77. M. Vatankhah-Varnosfaderani, A. N. Keith, Y. Cong, H. Liang, M. Rosenthal, M. Sztucki, C. Clair, S. Magonov, D. A. Ivanov, A. V. Dobrynin, S. S. Sheiko, *Science* **2018**, *359*, 1509.
78. B. B. Patel, D. J. Walsh, D. H. Kim, J. Kwok, B. Lee, D. Guironnet, Y. Diao, *Sci. Adv.* **2020**, *6*, eaaz7202.
79. G. M. Miyake, V. A. Piunova, R. A. Weitekamp, R. H. Grubbs, *Angew. Chem., Int. Ed.* **2012**, *51*, 11246.
80. P. G. O'Brien, D. P. Puzzo, A. Chutinan, L. D. Bonifacio, G. A. Ozin, N. P. Kherani, *Adv. Mater.* **2010**, *22*, 611.
81. D. Schneider, F. Liaqat, E. H. E. Boudouti, Y. E. Hassouani, B. Djafari-Rouhani, W. Tremel, H.-J. Butt, G. Fytas, *Nano Lett.* **2012**, *12*, 3101.
82. F. M. Hinterholzinger, A. Ranft, J. M. Feckl, B. Ruhle, T. Bein, B. V. Lotsch, *J. Mater. Chem.* **2012**, *22*, 10356.
83. N. Hidalgo, M. E. Calvo, M. G. Bellino, G. J. A. A. Soler-Illia, H. Míguez, *Adv. Funct. Mater.* **2011**, *21*, 2534.
84. L. Zhang, Z. Xiong, L. Shan, L. Zheng, T. Wei, Q. Yan, *Small* **2015**, *11*, 4910.
85. S. Liang, Y. Guan, Y. Zhang, *ACS Omega* **2019**, *4*, 5650.
86. T. Razaulla, M. Bekeris, H. Feng, M. Beeman, U. Nze, R. Warren, *Langmuir* **2021**, *37*, 12419.
87. J. B. Kim, G. H. Lee, S.-H. Kim, *ACS Appl. Mater. Interfaces* **2019**, *11*, 45237.
88. J. Vialetto, S. Rudiuk, M. Morel, D. Baigl, *J. Am. Chem. Soc.* **2021**, *143*, 11535.
89. N. L. Smith, A. Coukouma, S. Dubnik, S. A. Asher, *Phys. Chem. Chem. Phys.* **2017**, *19*, 31813.
90. W. Wang, B. Gu, *J. Phys. Chem. B* **2005**, *109*, 22175.
91. J. Yu, L. Zheng, C. Geng, X. Wang, Q. Yan, X. Wang, G. Shen, D. Shen, *Thin Solid Films* **2013**, *544*, 557.
92. A. R. Tao, J. Huang, P. Yang, *Acc. Chem. Res.* **2008**, *41*, 1662.
93. P. Jiang, M. J. McFarland, *J. Am. Chem. Soc.* **2004**, *126*, 13778.
94. B. G. Prevo, O. D. Velev, *Langmuir* **2004**, *20*, 2099.
95. H. Fudouzi, *Colloids Surf., A* **2007**, *311*, 11.
96. R. D. Deegan, O. Bakajin, T. F. Dupont, G. Huber, S. R. Nagel, T. A. Witten, *Nature* **1997**, *389*, 827.
97. H. Hu, R. G. Larson, *J. Phys. Chem. B* **2006**, *110*, 7090.
98. M. H. Kim, S. H. Im, O. O. Park, *Adv. Funct. Mater.* **2005**, *15*, 1329.
99. H. Yang, P. Jiang, *Langmuir* **2010**, *26*, 13173.
100. C.-Y. Cai, K.-Y. A. Lin, H. Yang, *Appl. Phys. Lett.* **2014**, *105*, 201913.
101. T. Ruhl, P. Spahn, G. P. Hellmann, *Polymer* **2003**, *44*, 7625.
102. T. Ruhl, G. P. Hellmann, *Macromol. Chem. Phys.* **2001**, *202*, 3502.
103. P. Wu, X. Shen, C. G. Schäfer, J. Pan, J. Guo, C. Wang, *Nanoscale* **2019**, *11*, 20015.
104. K. T. Hufziger, A. B. Zrimsek, S. A. Asher, *ACS Appl. Nano Mater.* **2018**, *1*, 7016.
105. A. Mikosch, S. Ciftci, G. Tainter, R. Shivanna, B. Haehnle, F. Deschler, A. J. C. Kuehne, *Chem. Mater.* **2019**, *31*, 2590.
106. Y. Suh, Q. Pham, B. Shao, Y. Won, *Small* **2019**, *15*, 18 04523.
107. S. H. Im, M. H. Kim, O. O. Park, *Chem. Mater.* **2003**, *15*, 1797.
108. A. S. Dimitrov, K. Nagayama, *Langmuir* **1996**, *12*, 1303.
109. Z.-Z. Gu, H. Uetsuka, K. Takahashi, R. Nakajima, H. Onishi, A. Fujishima, O. Sato, *Angew. Chem., Int. Ed.* **2003**, *42*, 894.
110. N. N. Khanh, K. B. Yoon, *J. Am. Chem. Soc.* **2009**, *131*, 14228.
111. S. Arpiainen, F. Jonsson, J. R. Dekker, G. Kocher, W. Khunsin, C. M. S. Torres, J. Ahopelto, *Adv. Funct. Mater.* **2009**, *19*, 1247.
112. Y. Yin, Y. Xia, *Adv. Mater.* **2001**, *13*, 267.
113. Y. Yin, Y. Lu, Y. Xia, *J. Am. Chem. Soc.* **2001**, *123*, 771.
114. H.-L. Li, W. Dong, H.-J. Bongard, F. Marlow, *J. Phys. Chem. B* **2005**, *109*, 9939.
115. H.-L. Li, F. Marlow, *Chem. Mater.* **2005**, *17*, 3809.
116. S.-H. Kim, S.-J. Jeon, W. C. Jeong, H. S. Park, S.-M. Yang, *Adv. Mater.* **2008**, *20*, 4129.
117. B. Ye, H. Ding, Y. Cheng, H. Gu, Y. Zhao, Z. Xie, Z. Gu, *Adv. Mater.* **2014**, *26*, 3270.
118. X. Zhao, Y. Cao, F. Ito, H.-H. Chen, K. Nagai, Y.-H. Zhao, Z.-Z. Gu, *Angew. Chem., Int. Ed.* **2006**, *45*, 6835.
119. Y. Zhao, Z. Xie, H. Gu, L. Jin, X. Zhao, B. Wang, Z. Gu, *NPG Asia Mater.* **2012**, *4*, e25.
120. Y. Cheng, F. Zheng, J. Lu, L. Shang, Z. Xie, Y. Zhao, Y. Chen, Z. Gu, *Adv. Mater.* **2014**, *26*, 5184.
121. N. P. Levenhagen, M. D. Dadmun, *Macromolecules* **2019**, *52*, 6495.
122. H. K. Raut, H. Wang, Q. Ruan, H. Wang, J. G. Fernandez, J. K. W. Yang, *Nano Lett.* **2021**, *21*, 8602.
123. J. Liao, C. Ye, J. Guo, C. E. Garciamendez-Mijares, P. Agrawal, X. Kuang, J. O. Japo, Z. Wang, X. Mu, W. Li, T. Ching, L. S. Mille, C. Zhu, X. Zhang, Z. Gu, Y. S. Zhang, *Mater. Today* **2022**, *56*, 29.
124. G.-R. Yi, J. H. Moon, S.-M. Yang, *Adv. Mater.* **2001**, *13*, 1185.
125. M. E. Leunissen, H. R. Vutukuri, A. van Blaaderen, *Adv. Mater.* **2009**, *21*, 3116.
126. F. Ma, S. Wang, L. Smith, N. Wu, *Adv. Funct. Mater.* **2012**, *22*, 4334.
127. J. Kleinert, S. Kim, O. D. Velev, *Langmuir* **2010**, *26*, 10380.
128. Y. Fang, W. Fei, X. Shen, J. Guo, C. Wang, *Mater. Horiz.* **2021**, *8*, 2079.
129. Z. Li, C. Qian, W. Xu, C. Zhu, Y. Yin, *Sci. Adv.* **2021**, *7*, eabh1289.
130. Y. Hu, L. He, Y. Yin, *Angew. Chem., Int. Ed.* **2011**, *50*, 3747.
131. T. M. Choi, K. Je, J.-G. Park, G. H. Lee, S.-H. Kim, *Adv. Mater.* **2018**, *30*, 1803387.
132. Y. Wu, R. Sun, J. Ren, S. Zhang, S. Wu, *Adv. Funct. Mater.* **2023**, *33*, 2210047.
133. L. Li, J. Xu, X. Lyu, Z. Liu, Z. Song, J. Wei, *Chem. Commun.* **2022**, *58*, 10032.

134. F. Liu, S. Zhang, Y. Meng, B. Tang, *Small* **2020**, *16*, 2002319.
135. S. Jung, K. I. MacConaghy, J. L. Kaar, M. P. Stoykovich, *ACS Appl. Mater. Interfaces* **2017**, *9*, 27927.
136. H. Sugiyama, T. Sawada, H. Yano, T. Kanai, *J. Mater. Chem. C* **2013**, *1*, 6103.
137. G. Wu, Y. Jiang, D. Xu, H. Tang, X. Liang, G. Li, *Langmuir* **2011**, *27*, 1505.
138. X. Xie, Z. Zhang, Q. Jiang, S. Zheng, Y. Yun, H. Wu, C. Li, F. Tian, M. Su, F. Li, *ACS Nano* **2022**, *16*, 20094.
139. Y. Yang, Y. Chen, Z. Hou, F. Li, M. Xu, Y. Liu, D. Tian, L. Zhang, J. Xu, J. Zhu, *ACS Nano* **2020**, *14*, 16057.
140. S. Li, Y. Zeng, W. Hou, W. Wan, J. Zhang, Y. Wang, X. Du, Z. Gu, *Mater. Horiz.* **2020**, *7*, 2944.
141. K. Matsubara, M. Watanabe, Y. Takeoka, *Angew. Chem., Int. Ed.* **2007**, *46*, 1688.
142. S. S. Lee, B. Kim, S. K. Kim, J. C. Won, Y. H. Kim, S.-H. Kim, *Adv. Mater.* **2015**, *27*, 627.
143. Y.-J. Quan, Y.-G. Kim, M.-S. Kim, S.-H. Min, S.-H. Ahn, *ACS Nano* **2020**, *14*, 5392.
144. M. Kolle, A. Lethbridge, M. Kreysing, J. J. Baumberg, J. Aizenberg, P. Vukusic, *Adv. Mater.* **2013**, *25*, 2239.
145. C. G. Schäfer, D. A. Smolin, G. P. Hellmann, M. Gallei, *Langmuir* **2013**, *29*, 11275.
146. B. Viel, T. Ruhl, G. P. Hellmann, *Chem. Mater.* **2007**, *19*, 5673.
147. J. M. Clough, J. Gucht, T. E. Kodger, Joris Sprakel, *Adv. Funct. Mater.* **2020**, *30*, 2002716.
148. P. Snapp, P. Kang, J. Leem, S. W. Nam, *Adv. Funct. Mater.* **2019**, *29*, 1902216.
149. Y. Guan, H. Li, S. Zhang, W. Niu, *Adv. Funct. Mater.* **2023**, *33*, 2215055.
150. H. Fudouzi, T. Sawada, *Langmuir* **2006**, *22*, 1365.
151. T. Ito, C. Katsura, H. Sugimoto, E. Nakanishi, K. Inomata, *Langmuir* **2013**, *29*, 13951.
152. H. Ding, C. Liu, H. Gu, Y. Zhao, B. Wang, Z. Gu, *ACS Photonics* **2014**, *1*, 121.
153. S. Wang, W.-Y. Wu, J. C. C. Yeo, X. Y. D. Soo, W. Thitsartarn, S. Liu, B. H. Tan, A. Suwardi, Z. Li, Q. Zhu, X. J. Loh, *BMEMat* **2023**, *1*, e12021.
154. Q. Yang, S. Zhu, W. Peng, C. Yin, W. Wang, J. Gu, W. Zhang, J. Ma, T. Deng, C. Feng, D. Zhang, *ACS Nano* **2013**, *7*, 4911.
155. C. Li, B. V. Lotsch, *Chem. Commun.* **2012**, *48*, 6169.
156. A. C. Sharma, T. Jana, R. Kesavamoorthy, L. Shi, M. A. Virji, D. N. Finegold, S. A. Asher, *J. Am. Chem. Soc.* **2004**, *126*, 2971.
157. J. Shin, P. V. Braun, W. Lee, *Sens. Actuators, B* **2010**, *150*, 183.
158. H. Huang, H. Li, J. Yin, K. Gu, J. Guo, C. Wang, *Adv. Mater.* **2023**, *35*, 2211117.
159. J. Hu, S. Yang, Z. Chen, Y. Chen, J. Wei, *ACS Appl. Polym. Mater.* **2023**, *5*, 1002.
160. Y. Qiu, Y. Yang, C. Valenzuela, X. Zhang, M. Yang, P. Xue, J. Ma, Z. Liu, L. Wang, W. Feng, *Adv. Opt. Mater.* **2022**, *10*, 2102475.
161. Z.-Y. Xie, L.-G. Sun, G.-Z. Han, Z.-Z. Gu, *Adv. Mater.* **2008**, *20*, 3601.
162. H. S. Lim, J.-H. Lee, J. J. Walish, E. L. Thomas, *ACS Nano* **2012**, *6*, 8933.
163. M. Lu, X. Zhang, D. Xu, N. Li, Y. Zhao, *Adv. Mater.* **2023**, *35*, 2211330.
164. I. B. Burgess, L. Mishchenko, B. D. Hatton, M. Kolle, M. Loncar, J. Aizenberg, *J. Am. Chem. Soc.* **2011**, *133*, 12430.
165. Y. Chen, Z. Zuo, Z. Liu, Y. Yin, *Small* **2022**, *18*, 2204484.
166. X. Hu, J. Huang, W. Zhang, M. Li, C. Tao, G. Li, *Adv. Mater.* **2008**, *20*, 4074.
167. W. Hong, X. Hu, B. Zhao, F. Zhang, D. Zhang, *Adv. Mater.* **2010**, *22*, 5043.
168. J. Cui, W. Zhu, N. Gao, J. Li, H. Yang, Y. Jiang, P. Seidel, B. J. Ravoo, G. Li, *Angew. Chem., Int. Ed.* **2014**, *53*, 3844.
169. J. H. Holtz, S. A. Asher, *Nature* **1997**, *389*, 829.
170. H. Saito, Y. Takeoka, M. Watanabe, *Chem. Commun.* **2003**, *17*, 2126.
171. B.-F. Ye, Y.-J. Zhao, Y. Cheng, T. T. Li, Z.-Y. Xie, X.-W. Zhao, Z.-Z. Gu, *Nanoscale* **2012**, *4*, 5998.
172. B. Ye, F. Rong, H. Gu, Z. Xie, Y. Cheng, Y. Zhao, Z. Gu, *Chem. Commun.* **2013**, *49*, 5331.
173. V. L. Alexeev, S. Das, D. N. Finegold, S. A. Asher, *Clin. Chem.* **2004**, *50*, 2353.
174. K. I. MacConaghy, C. I. Geary, J. L. Kaar, M. P. Stoykovich, *J. Am. Chem. Soc.* **2014**, *136*, 6896.
175. Z. Tian, Z. Zhang, D. Zhang, D. Yang, C. Cao, S. Huang, *ACS Appl. Nano Mater.* **2022**, *5*, 12787.
176. P. Ren, X. Chen, L. Sun, Q. Lyu, L. Zhang, J. Zhu, *ACS Appl. Mater. Interfaces* **2022**, *14*, 50190.
177. H. Hu, Q.-W. Chen, H. Wang, R. Lia, W. Zhong, *J. Mater. Chem.* **2011**, *21*, 13062.
178. X. Ye, Y. Li, J. Dong, J. Xiao, Y. Ma, L. Qi, *J. Mater. Chem. C* **2013**, *1*, 6112.
179. H. Fudouzi, Y. Xia, *Adv. Mater.* **2003**, *15*, 892.
180. J. Ge, J. Goebl, L. He, Z. Lu, Y. Yin, *Adv. Mater.* **2009**, *21*, 4259.
181. Z. Wang, J. Zhang, J. Xie, C. Li, Y. Li, S. Liang, Z. Tian, T. Wang, H. Zhang, H. Li, W. Xu, B. Yang, *Adv. Funct. Mater.* **2010**, *20*, 3784.
182. H. Yang, P. Jiang, *Appl. Phys. Lett.* **2011**, *98*, 011104.
183. Y. Zhang, J. Qiu, M. Gao, P. Li, L. Gao, L. Heng, B. Z. Tang, L. Jiang, *J. Mater. Chem. C* **2014**, *2*, 8865.
184. L. Bai, Z. Xie, W. Wang, C. Yuan, Y. Zhao, Z. Mu, Q. Zhong, Z. Gu, *ACS Nano* **2014**, *8*, 11094.
185. Z. Xie, K. Cao, Y. Zhao, L. Bai, H. Gu, H. Xu, Z.-Z. Gu, *Adv. Mater.* **2014**, *26*, 2413.
186. C.-H. Hsieh, F.-T. Lin, K.-Y. A. Lin, S.-Y. Hsieh, Y.-T. Chen, H.-P. Tsai, C.-H. Lu, H. Yang, *ACS Appl. Nano Mater.* **2022**, *5*, 15855.
187. Y. Jiang, D. Xu, X. Li, C. Lin, W. Li, Q. An, C. Tao, H. Tang, G. Li, *J. Mater. Chem.* **2012**, *22*, 11943.
188. S. Shibayama, H. Higuchi, Y. Okumura, H. Kikuchi, *Adv. Funct. Mater.* **2013**, *23*, 2387.
189. S. Kubo, Z. Gu, K. Takahashi, A. Fujishima, H. Segawa, O. Sato, *Chem. Mater.* **2005**, *17*, 2298.
190. G. Z. Han, Z. Y. Xie, D. Zheng, L. G. Sun, Z. Z. Gu, *Appl. Phys. Lett.* **2007**, *91*, 141114.
191. D. P. Puzzo, A. C. Arsenault, I. Manners, G. A. Ozin, *Angew. Chem., Int. Ed.* **2009**, *48*, 943.
192. G. A. Ozin, A. C. Arsenault, *Mater. Today* **2008**, *11*, 44.
193. A. C. Arsenault, D. P. Puzzo, I. Manners, G. A. Ozin, *Nat. Photonics* **2007**, *1*, 468.
194. M. G. Han, C. G. Shin, S.-J. Jeon, H. Shim, C.-J. Heo, H. Jin, J. W. Kim, S. Lee, *Adv. Mater.* **2012**, *24*, 6438.
195. T. S. Shim, S.-H. Kim, J. Y. Sim, J.-M. Lim, S.-M. Yang, *Adv. Mater.* **2010**, *22*, 4494.
196. I. Lee, D. Kim, J. Kal, H. Baek, D. Kwak, D. Go, E. Kim, C. Kang, J. Chung, Y. Jang, S. Ji, J. Joo, Y. Kang, *Adv. Mater.* **2010**, *22*, 4973.
197. Q. Fu, W. Yu, G. Bao, J. Ge, *Nat. Commun.* **2022**, *13*, 7007.
198. C. Zhu, W. Xu, L. Chen, W. Zhang, H. Xu, Z. Z. Gu, *Adv. Funct. Mater.* **2011**, *21*, 2043.

199. J. Ge, H. Lee, L. He, J. Kim, Z. Lu, H. Kim, J. Goebl, S. Kwon, Y. Yin, *J. Am. Chem. Soc.* **2009**, *131*, 15687.
200. Z. Li, M. Wang, X. Zhang, D. Wang, W. Xu, Y. Yin, *Nano Lett.* **2019**, *19*, 6673.
201. X. Xu, G. Friedman, K. D. Humfeld, S. A. Majetich, S. A. Asher, *Chem. Mater.* **2002**, *14*, 1249.
202. J. Ge, Y. Hu, T. Zhang, T. Huynh, Y. Yin, *Langmuir* **2008**, *24*, 3671.
203. J. Ge, Y. Hu, Y. Yin, *Angew. Chem., Int. Ed.* **2007**, *46*, 7428.
204. W. Luo, H. Ma, F. Mou, M. Zhu, J. Yan, J. Guan, *Adv. Mater.* **2014**, *26*, 1058.
205. X.-Q. Wang, C.-F. Wang, Z.-F. Zhou, S. Chen, *Adv. Opt. Mater.* **2014**, *2*, 652.
206. S. Sacanna, A. P. Philipse, *Langmuir* **2006**, *22*, 10209.
207. C. Zhu, L. Chen, H. Xu, Z. Z. Gu, *Macromol. Rapid Commun.* **2009**, *30*, 1945.
208. H. Kim, J. Ge, J. Kim, S. Choi, H. Lee, H. Lee, W. Park, Y. Yin, S. Kwon, *Nat. Photonics* **2009**, *3*, 534.
209. H. Lee, J. Kim, H. Kim, J. Kim, S. Kwon, *Nat. Mater.* **2010**, *9*, 745.
210. J. Ge, Y. Yin, *Adv. Mater.* **2008**, *20*, 3485.
211. H. Zhang, H. Chen, J.-H. Lee, E. Kim, K.-Y. Chan, H. Venkatesan, M. H. Adegun, O. G. Agbabiaka, X. Shen, Q. Zheng, J. Yang, J.-K. Kim, *Adv. Funct. Mater.* **2022**, *32*, 2208362.
212. Y. Chen, Z. Lou, Z. Chen, S. Yang, J. Hu, J. Wei, *Langmuir* **2022**, *38*, 14387.
213. M. Honda, T. Seki, Y. Takeoka, *Adv. Mater.* **2009**, *21*, 1801.
214. M. A. Haque, G. Kamita, T. Kurokawa, K. Tsujii, J. P. Gong, *Adv. Mater.* **2010**, *22*, 5110.
215. M. Chen, L. Zhou, Y. Guan, Y. Zhang, *Angew. Chem., Int. Ed.* **2013**, *52*, 9961.
216. J. Wang, Y. Hu, R. Deng, R. Liang, W. Li, S. Liu, J. Zhu, *Langmuir* **2013**, *29*, 8825.
217. Y. F. Yue, M. A. Haque, T. Kurokawa, T. Nakajima, J. P. Gong, *Adv. Mater.* **2013**, *25*, 3106.
218. J. Liao, C. Zhu, B. Gao, Z. Zhao, X. Liu, L. Tian, Y. Zeng, X. Zhou, Z. Xie, Z. Gu, *Adv. Funct. Mater.* **2019**, *29*, 1902954.
219. C. G. Schäfer, M. Gallei, J. T. Zahn, J. Engelhardt, G. P. Hellmann, M. Rehahn, *Chem. Mater.* **2013**, *25*, 2309.

AUTHOR BIOGRAPHIES

Cun Zhu received his PhD degree in 2013 from Southeast University. He started his career at the School of Biological Science and Medical Engineering, Southeast University in the same year. His research interests mainly focus on the fabrication of noble metal nanocrystals and photo-functional colloidal crystals with controllable morphologies for anti-counterfeiting and sensing.

Lei Tian received his PhD degree from McMaster University in June 2022. He is currently a Postdoc Fellow in Chemical Engineering, McMaster University. His research interests mainly focus on bacteriophage-built materials and microstructured hydrogels toward diverse biomedical applications, including antifouling surfaces, antimicrobial microparticles, and biosensors.

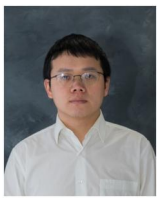

Wei Cheng received his PhD degree in 2014 from Shanghai Jiao Tong University. He started his career at the Department of Chemical and Biochemical Engineering, the University of Iowa in 2015. His research interests mainly focus on the fabrication of photo-functional materials such as semiconducting nanowires for novel solar conversion and storage systems.

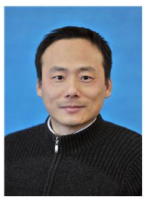

Zhongze Gu received his PhD degree in 1998 from the University of Tokyo under the direction of Professor Akira Fujishima. He then started his academic career at the Kanagawa Academy of Science and Technology as a researcher. Since 2003, he has been a Cheung Kong Scholars professor at Southeast University. He is now the dean of the School of Biological Science and Medical Engineering, Southeast University. His research interests include bio-inspired photonic materials, bioelectronic devices, and organ-on-a-chip for biomedical applications.

How to cite this article: C. Zhu, L. Tian, W. Cheng, Z. Gu, *BMEMat* **2024**, *2*(1), e12056. https://doi.org/10.1002/bmm2.12056